Student thesis series INES nr 291

GIS-based time series study of soil erosion risk using the Revised Universal Soil Loss Equation (RUSLE) model in a micro-catchment on Mount Elgon, Uganda

Boyi Jiang

2013
Department of Earth and Ecosystem Sciences
Physical Geography and Ecosystems Analysis
Lund University
Sölvegatan 12
S-223 62 Lund
Sweden

Boyi Jiang (2013). GIS-based time series study of soil erosion risk using the Revised Universal Soil Loss Equation (RUSLE) model in a micro-catchment on Mount Elgon, Uganda
Master degree thesis, 30 credits in *Geomatics*
Department of Physical Geography and Ecosystems Science, Lund University

GIS-based time series study of soil erosion risk using the Revised Universal Soil Loss Equation (RUSLE) model in a micro-catchment on Mount Elgon, Uganda

---

Boyi Jiang

Master Degree Thesis in Geomatics, 30 credits
Department of Physical Geography and Ecosystems Science
Lund University, Sweden, 2013

Supervisor

Petter Pilesjö

Lund University GIS Centre, Department of Physical Geography and Ecosystems Science
Lund University, Sweden, 2013

Co-supervisor

Yazidhi Bamutaze

Department of Geography, Geo-Informatics and Climatic Sciences,
College of Agricultural and Environmental Sciences (MCAES)
Makerere University, Uganda, 2013

Abstract

Land degradation has already been treated as one of the most serious problem all around the world. This study is a GIS-based time series study which devotes to calculate annual soil loss value, seek for soil erosion trends linked with precipitation and land use in Manafwa micro-catchment, Mount Elgon region, Uganda. Two different versions of Revised Universal Soil loss Equation (RUSLE) are implemented and compared, one using flow length and the other using flow accumulation to estimate the slope length and steepness (LS) factor. The modeling is carried out for the years 2000, 2006, and 2012, and is based on ASTER remotely sensed data, digital elevation models, precipitation data from the study area, as well as existing soil maps. After running RUSLE model and analyzing the result maps, no significant soil erosion trends or patterns are found, as well as significant trends in precipitation and land cover changes during last decade. Over exploitation of land is probably compensated by improved agricultural management and no significant increase in precipitation. Even if there are reports of more intense and increasing amounts of rainfall in the area, this could not be verified, neither through analysis of climate data, nor by trends in estimated soil loss.

Keywords: Soil erosion, Revised Universal Soil Loss Equation (RUSLE), GIS, Time series, Uganda

Table of Contents

List of Figures

List of Tables

Acknowledgements

I am really grateful for those persons that helped me a lot and provided me possibility to complete this master thesis:

To my supervisor Petter Pilesjö from Lund University GIS centre, Department of Physical Geography and Ecosystem Science, Lund University, Sweden, who guided me, gave me constructive suggestions during the whole process and improving the report and helped me solve problems carefully and patiently through the whole thesis work;

To my co-supervisor Yazidhi Bamutaze from Department of Geography, Geo-Informatics and Climatic Sciences, College of Agricultural and Environmental Sciences (MCAES) Makerere University, Uganda, who provided DEM data, climate data, original soil map, and some relative local literatures to support this study, also gave me good suggestions and helped me with improving the report;

To all my friends and families, who support and encourage me through the whole thesis project.

Lund, 27th August, 2013
Boyi Jiang

1. Introduction

1.1 Background

As one of the most important basic natural resource, land relates to almost all the human activities directly or indirectly, and is crucial for sustaining livelihoods in many Sub Saharan African (SSA) countries. Rational utilization of the land resource has been treated as the key factor in the development pathways of many SSA countries. However, land degradation is one of the major and widespread environmental threats both in the past and present years (Xu et al., 2012). Furthermore, soil erosion is regarded as the most serious form of land degradation around the world, especially in developing countries like Uganda, China and India as well as some developed countries like Spain (Brunner et al., 2004; Nekhay et al., 2009; Zhang et al., 2010). In order to meet their livelihoods, address the economic stress and accelerate development, some people and development actors in the developing countries utilize land and soil resource in unsustainable and irrational ways as manifested by overgrazing, destruction of forest for urban extension, heavy intensity and unscientific agricultural activities, land use changes in high-frequency (De Meyer et al., 2011). As the result, soil erosion becomes seriously, which negatively impacts the soil quality reducing agricultural efficiency, worsening water quality, flooding, debris flow and habitat destruction (Park et al., 2011).

Mountain ecosystems are considered as one of the most significant ecosystems, providing huge amount of benefits to human both in natural aspect and economic aspects via various ecosystem services and products. Nevertheless, unsustainable and unscientific land use practices and improper land management causes serious soil erosion in mountain regions. More and more studies are carried out focusing on the mountainous areas in order to get better understanding about why the phenomenon happens and what could be done to solve the problems (Bamutaze et al., 2010; Mugagga et al., 2012; Soini, 2005; Prasannakumar et al., 2012). In recent years, governments started to pay attention to sustainable agriculture and development. As the result, many environment and land degradation assessment policies are announced and published, which points out that soil erosion and land degradation in the mountain areas are increasingly regarded more serious than in other ecosystems (NEMA, 1998; Millward & Mersey, 1999; Angima, 2003; Jasrotia & Singh, 2006). One of the major reasons for this is land use changes in high-frequency, not only modifications, but also conversion of the land cover, which has negative impact on the environment, especially replacement of the forests area by agriculture fields due to the pressure of population (Hansen et al., 2001; Lung & Schaab, 2010). The other major reason is the irregular terrain and topography in the mountain areas, which means that the slope

diversity and heterogeneity are significant factors for the intensity of soil erosion (Knapen et al., 2006). Combined with rapid climate variability and changes, mountain ecosystems are one of the most sensitive ecosystems to climate change. The variation in rainfall pattern significantly impacts the runoff.

In a study by Knapen et al. (2006), carried out on Mount Elgon in Uganda, it was observed that East Africa has severe land degradation around the highlands. They also point out that high vulnerability of the slopes, the high annual precipitation, including steep slope and high weathering rates, can be the important reasons for the serious soil erosion in this area. In the end of their report, the human activities due to high population density and associated pressures are considered as the most important factor for the land degradation. Another study which focused on land use changes around Mount Elgon done by Mugagga et al. (2012) indicates that population pressure in the Mount Elgon region has resulted in large areas of forest being replaced by agriculture fields without sustainable management. These unsustainable and unscientific land use practices have caused a lot of environmental problems exemplified by landslides, high erosion rates and stream pollution loading on Mount Elgon. It is however decided that activities supporting forest replacement by cropland and grazing land will continue until 2032 (UNEP, 2004).

East Arica has been emphasized as the focal point of soil erosion. Better management and sustainable development measures have to be worked out and implemented.

There are two main approaches to study the soil erosion, depending on spatial and temporal scales (Xu et al., 2012). One entails on-site measurements, which perform irrigation experiments on small scale plots. The other is the off-site quantification through modeling, which can be applied to reveal potential patterns of the soil erosion, or evaluate the soil erosion on a large scale. According to Rafaelli et al. (2001), if data from field measurements are lacking and sparse due to costs of manpower and time constraints, off-site modeling techniques are to prefer. Lack of data is apparent in the Mount Elgon region, partly due to climate conditions, with a high cloud cover, and partly due to the location, with steep slopes and a spare road network making it difficult and expensive to carry out field measurements.

In order to build the quantification model, as many as possible of the criteria which influence soil erosion should be taken into consideration. The Revised Universal Soil Loss Equation (RUSLE) is a widely used soil erosion intensity evaluation model, modified and improved from the Universal Soil Loss Equation (USLE), developed by Wischmeier (1976). There are several factors included in this model, such as rainfall erosivity, soil erodability, slope length and steepness factor, cover management factor,

and conservation practice factor. RUSLE can be treated as a kind of multi-criteria analysis, since the results are calculated according to the influencing factors. GIS technology is thus appropriate due to its powerful multi-criteria processing and calculation capability (Chretien et al., 1994; Fu & Gulinck, 1994). Moreover, in many conclusions of previous studies, highly significant spatio-temporal phenomena or changing patterns are revealed by applying GIS and remote sensing based soil erosion and land degradation modeling (Fistikoglu & Harmancioglu, 2002; Hoyos, 2005). Long term studies can be performed, and the changes in soil erosion intensity patterns can be shown and analyzed. Hence, evaluation and prediction are possible to carry out much easier and faster than before to address hazards caused by soil erosion.

1.2 Aims and objectives

The first specific aim is thus to produce high accuracy soil erosion estimates for the study area. Secondly, possible climate and soil erosion intensity trends from 2000 to 2012 are discussed. The original RUSLE model structure is compared with an updated RUSLE model, where the slope length factor is replaced by drainage area. If the evaluation shows the updated RUSLE model to be more accurate, the model has been improved. These aims are addressed through the following objectives:

- To understand the influencing factors in the RUSLE model and the basic usage of the model by reviewing literature and previous studies.
- To perform the two different model calculations for the years 2000, 2006 and 2012 in order to estimate soil erosion and create soil erosion intensity maps.
- To compare the accuracy of the two methods and choose a more reliable results for discussion.
- To analyze and discuss the results of possible soil erosion intensity trend from the year 2000 to 2012, affecting by precipitation and land cover situation in the study area.

1.3 Research questions

The major questions which the study attempted to address are:

- Is the updated version of RUSLE, using flow accumulation instead of slope length, to prefer?
- How much soil is lost each year during the last decade in the selected micro-catchment on Mount Elgon?

- What is the soil erosion pattern from the year 2000 to 2012?

1.4 General methodology and organization of the thesis

In order to answer the research questions, several steps were undertaken. Firstly, relevant literature was reviewed, including basic information about Uganda and the certain study area, the factors in the RUSLE model, and knowledge about previous use of the model. Secondly, referring to the factors in the model, the datasets of the study area were collected from various sources. Digital elevation models (DEM), satellite images, climate data for rainfall, and soil classification map were used. Afterwards, by applying the RUSLE model and the updated RUSLE model, the result of soil erosion intensity of the target years were estimated and presented in tabular formats as well as maps. Finally, a comparison was performed to assess the accuracy of the results derived using the original RUSLE structure and the modified structure. A statistical analysis was carried out in order to explain possible soil erosion patterns and trends as well as the climate influence.

As the results, six thematic maps presenting soil erosion intensity were obtained, two for each year, as well as the figures showing the percentage of coverage for each of the erosion risk level. According to the result maps, the reasons for the differences are expected to be found and discussed. Statistic analysis and evaluation will be helpful to find those reasons and have a quantitative explanation about soil erosion patterns.

This thesis is organized in seven chapters. As presented before, Introduction Chapter gives the background information about soil erosion study field and presents aims and objectives of this study. Study Area Chapter introduces the basic information like location, topography, climate, soil, vegetation cover and land use of the studied micro-catchment. In Materials Chapter, series of the data used in this study are provided and introduced with the explanation of the data sources and relevant parameters. Methodologies Chapter illustrates the whole RUSLE modeling and detailed explanation about each factor computation. Results and Discussion Chapter presents six thematic maps showing soil erosion intensity obtained by two different methods and the comparison between the methods. Additionally, the limitations and difficulties are discussed and pointed out, as well as the relationships among annual soil loss, precipitation and land cover changes. Finally, Conclusion Chapter summarizes the work done from data collection to final results, as well emphasize the limitations and difficulties and gives simple perspectives for future studies.

2. Study Area

2.1 Location

The study area is located on the Ugandan territory of Mount Elgon. Mount Elgon is a transboundary mountain which lies on the border of western Kenya and eastern Ugandan. Mount Elgon can be regarded as the largest and oldest extinct volcano from Pliocene age in East Africa. The elevation is about 4322 meters (Claessens et al., 2007). The actual study area constitutes part of Manafwa catchment, lying on the western side as illustrated in the Figure 1 below. The map below shows the position of the study area. It is located between latitude 0.893 ° and 1.084 °, and longitude 34.056 ° and 34.384 ° in WGS84 coordinates system. The total coverage of the study area is 365 km^2.

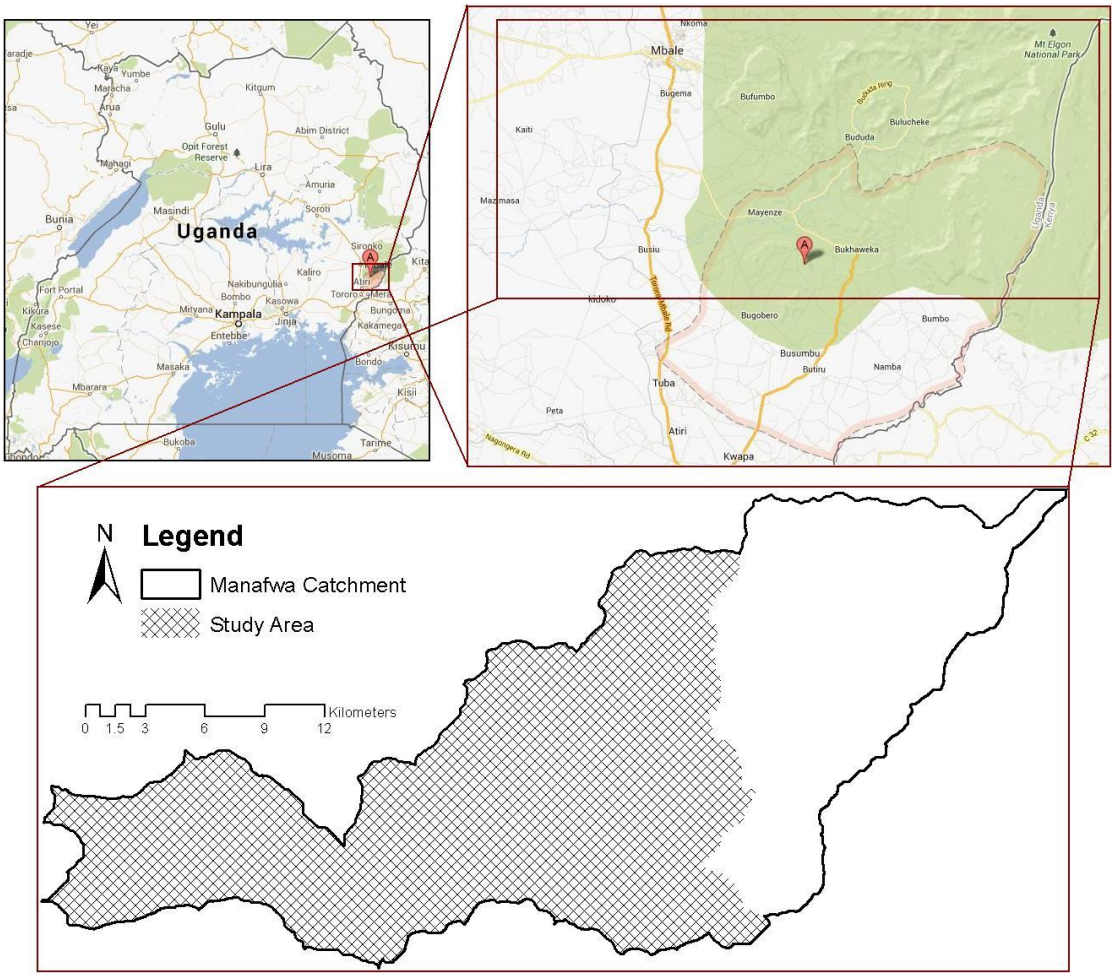

Figure 1. Location for the study area.

2.2 Topography

Several studies point out that the geomorphology of the Mount Elgon region is dominated by volcanism (Kitutu et al., 2009; Knapen et al., 2006). The elevation in the study area varies between 1084 and 2455 meters. Due to mountainous characteristics, the variation of the slope is large. The largest slope is 50 degree, 48% of the area have slopes less than 5 degrees, 18% of the area have slopes from 5 to 10 degrees, 23% of the area have slopes between 10 and 20 degrees, and 11% of the study area have slopes exceeding 20 degrees.

2.3 Climate

The climate of Mount Elgon region can be defined as humid subtropical. It is dominated by seasonally alternating moist Southwesterly and dry Northeasterly air streams. The mean annual air temperature is about 23 ℃. Moreover, average minimum and maximum temperature is 15 ℃ and 28 ℃, respectively. The warmest months in the year are from January to March and the coolest months are from July to August. The onset and cessation of rainfall months are March and December, respectively. The mean annual precipitation is generally high around 1500 mm (Bamutaze et al., 2010). The precipitation in Mount Elgon region shows a weak bi-modal pattern. The rainfall differences are mostly influenced by orographic conditions, altitude and location. Specifically, in Bamutaze (2010), a long term analysis of rainfall pattern for Bududa station which is located in west part of the study area shows a weak bio-modal precipitation distribution of the study area. Figure 2 indicates, the two rainy seasons in the year are somewhere around May and August.

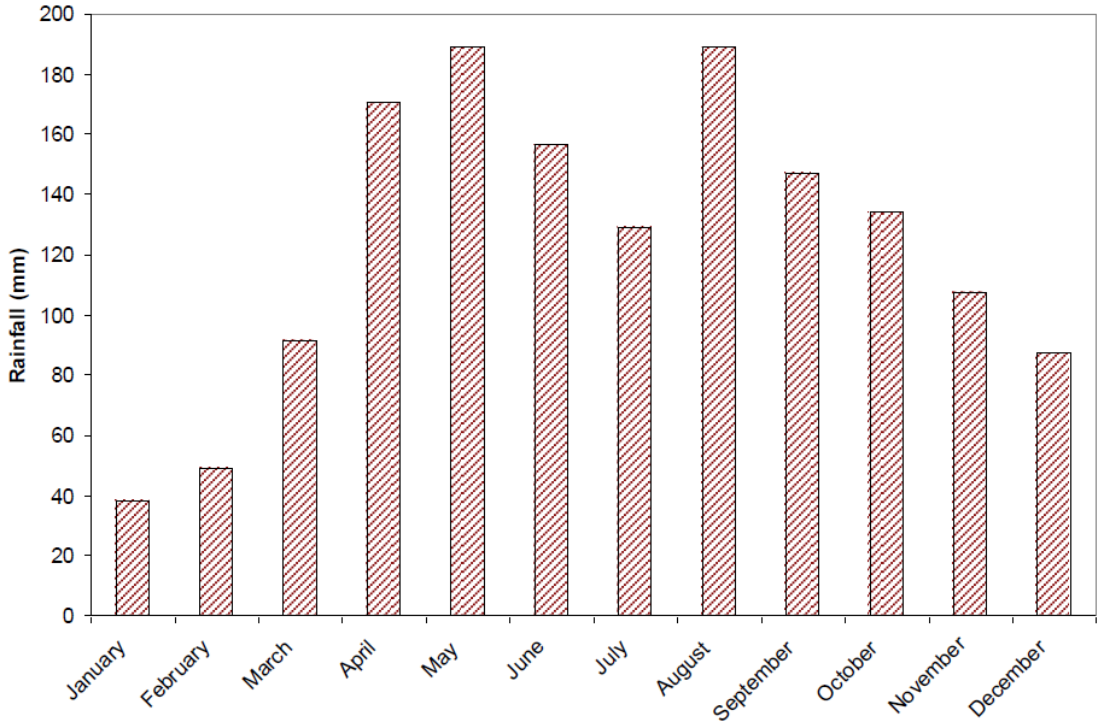

Figure 2. Mean monthly rainfall distribution for Bududa station (Bamutaze, 2010).

2.4 Soil

Generally, the soil structure of Mount Elgon is deep and derived from volcanic ash as the product of a single weathering cycle (NEMA, 1998). A significant characteristic pointed out by Isabirye (2004) is that the soils of this area are highly variable cause of the structure of the carbonatite dome. In the study done by Bamutaze (2010), three main sources of the soil types in Mount Elgon are stated. Firstly, volcanic ash and agglomerate found under volcanic mountains and hills and the pediments of them have contributed to derive the soils. Secondly, some of the soils are derived from metamorphic rocks, which are the degraded Gondwana surface. Thirdly, another part of soils is derived from mixed volcanic-metamorphic rocks.

2.5 Vegetation and land cover

The distribution of vegetation in Mount Elgon region is influenced by many physical and anthropogenic factors, such as, elevation, aspect, soil, climate, and land use practices (Wesche, 2002). Generally, four different broad vegetation communities can be observed. Mixed montane forest can be found up to elevation of 2500 meters, bamboo and canopy montane forest can be found from 2400 to 3000 meters, and moorland can be found above 3500 meters (Scott, 1994). However, the natural

vegetation is heavily influenced by human activities. Because of the pressure from the rapidly increasing population, natural vegetation is damaged by intense agriculture and grazing activities, especially in the area below 2200 meters. Agriculture lands occupy 47% of the landscape, and grassland areas cover 22% (Van Heist, 1994). This potential damage of the ground cover vegetation of course can lead to an increased risk of soil erosion.

2.6 Population and land use

The estimated population density of Manafwa catchment region varies between 250 and 700 persons per square kilometer (Bamutaze et al., 2010). The land use types in the Mount Elgon region can be classified as crop lands, secondary forest, natural forest, bare land and built up areas. Agriculture lands are the most common land use type across this area and agriculture activities are extremely frequent (Van Heist, 1994). The agriculture activities are mostly carried out below the elevation 2000 meters. Montane farming system and smallholdings are the most common forms of the agriculture in this region (Wasige, 2007). Due to low efficiency of the agriculture and the huge pressure caused by the population, the crop lands encroach higher mountain area, which can impact on the natural forest area. Mugagga et al. (2012) note that the most significant land use changes are the conversion from natural forest to other land use types, especially crop lands and grazing lands. This kind of land management can easily lead to increased land degradation and soil erosion.

3. Materials

3.1 Digital elevation model

Terrain data required for the modeling (flow length, flow accumulation, slope gradient etc) were all extracted from a DEM. This original DEM was provided and interpolated from a 10 meters resolution contours map by Department of Mapping and Surveys for Uganda. The extracted raster DEM was generated in ArcGIS 10 by using the inherent protocols. It is under WGS 1984 spatial reference coordinates system and projected to UTM Zone 36N projection system. The spatial resolution is 25 meters. The elevation range of the Mount Elgon region is from 1041 meters up to 4301 meters. The DEM data were used to estimate slope gradient, flow direction, catchment area, flow length and flow accumulation for the study.

3.2 Climate data

The climate data are from Bamutaze (2010), collecting from four different climate stations: Bududa, Bulucheke, Buwabwale and Nabumali. The position of the climate stations and the location of the study area are shown below in Figure 3. The rainfall data are obtained from the Department of Meteorology of Uganda. The climate data include precipitation, relative humidity, solar intensity, wind speed and temperature. All the data are provided in DBF format, which can be read as tables by ArcGIS 10 or Excel.

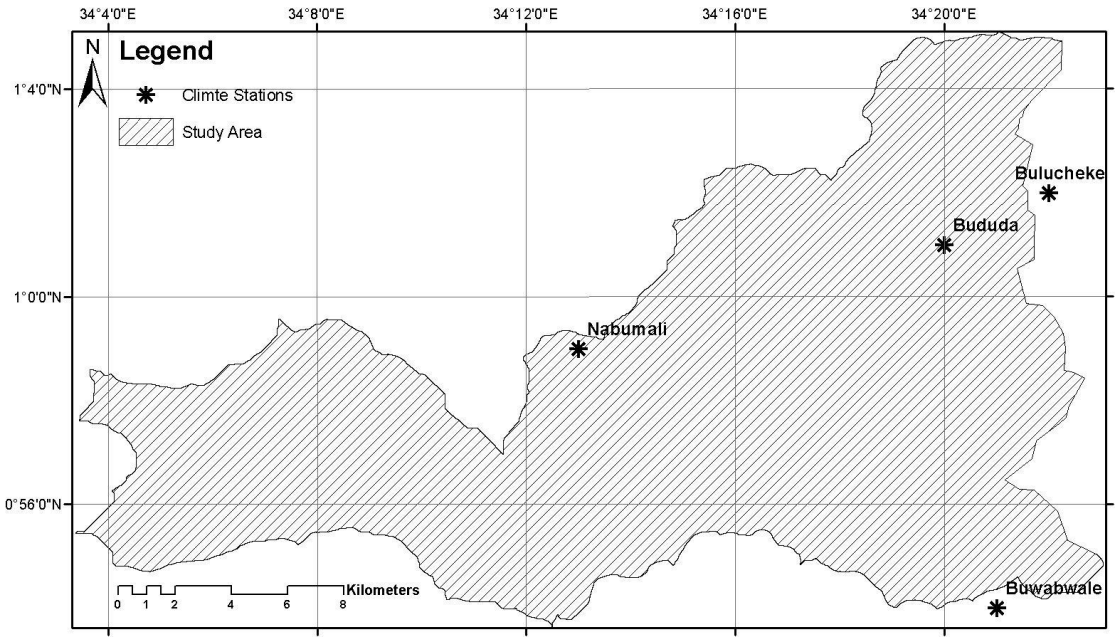

Figure 3. Location of the climate stations and the study area.

Only precipitation is interesting for this study. The data are distributed in daily form. The rainfall depth data in millimeter for the target years 2000, 2006 and 2012 were extracted from a large dataset. The precision of this dataset is 0.01 millimeters. The rainfall erosivity factor was estimated by interpolating the values from these climate stations.

3.3 Soil data

Due to limitations in the available soil data, a combination of two different types of soil data was used in this study. Two soil maps which contain different soil types as attributes are used (Bamutaze, 2010). The soil types are in FAO (Food and Agriculture Organization) classification system. One soil map contains more detailed soil information of the area located in southwest part of Mount Elgon region. Unfortunately, there are some gaps in the data. In order to fill these gaps, another Uganda nation level soil map with lower resolution was used to make updating and correcttions. As a result, a full soil map of southwest Mount Elgon was generated to aid the estimation of the soil erodability factor.

3.4 Satellite remote sensing images

The used ASTER satellite images are from the summer period of the years 2000, 2006 and 2012.

The spatial resolution of the satellite images are 15 meters. All images were geo-referenced under the WGS84 coordinate system. Detailed information about the used ASTER images is shown in Table 1. The three satellite images used are expected to be from the same date. However, due to the heavy cloud coverage in Mount Elgon region during summer time, this requirement is difficult to fulfill. The data used in this study are the best combination which can be found. The detailed explanation and discussion is presented in the discussion section.

Table 1. The instruction for the ASTER images.

Product ID	Time	Central Coordinates	Cloud Coverage	Bands
prodat011	2012/6/27	Lat: 1.107, Long: 34.261	20%	Band1, Band2, Band3N
prodat012	2006/8/30	Lat: 1.111, Long: 34.236	13%	Band1, Band2, Band3N
prodat013	2000/9/30	Lat: 1.124, Long: 34.144	4%	Band1, Band2, Band3N

There are three bands in the downloaded data, BAND1, BAND2, and BAND3N. The corresponding wave lengths of the three bands are shown in Table 2.

Table 2. The wave length for each of the bands in VNIR subsystem for ASTER.

Band No.	Wave length (μm)	Color
1	0.52-0.60	Green
2	0.63-0.69	Red
3N	0.78-0.86	Near-infrared

In the downloaded data, the digital values for Green, Red and Near-infrared band were interpreted following the spectral reflectance characteristics. That means the satellite images can be used for NDVI calculation directly in the further processing stage. The NDVI maps indicate the land cover environment. NDVI was thus used to estimate the cover management factor which is one of the components in RUSLE model.

3.5 Field data

Field measurements of soil erosion collected and presented by Bamutaze (2010) are used in this study. Soil loss was measured in field at eleven different locations in the study area. All measurements were carried out by the use of sediment traps in open streams.

4. Methodologies

4.1 The RUSLE model

The RUSLE soil erosion model is used to estimate annual soil loss value and estimate soil erosion intensity in a catchment. The RUSLE model is based on the USLE erosion model structure which was developed by Wischmeier & Smith (1978), and improved and modified by Renard et al. (1997). Five parameters are used in the RUSLE model to estimate soil loss. They are rainfall erosivity (R), soil erodability (K), slope length and steepness factor (LS), cover management factor (C) and conservation practice factor (P). Referring to RUSLE model, the relationship is expressed as:

$$A = R \times K \times LS \times C \times P \quad (1)$$

where A ($t\,ha^{-1}\,y^{-1}$) is the computed spatial average of total soil loss per year; R ($MJ\,mm\,ha^{-1}\,h^{-1}y^{-1}$) is the rainfall erosivity factor; K ($t\,ha\,h\,ha^{-1}\,MJ^{-1}\,mm^{-1}$) is the soil erodability factor; LS is the slope length and steepness factor (dimensionless); C is the land surface cover management factor (dimensionless); and P is the erosion control or called conservation practice factor (dimensionless).

The methods and formulas for estimating each of the parameters in the RUSLE model are mainly based on three previous studies by Bamutaze (2010), Pilesjö (1992) and Prasannakumar et al. (2012). The work flow is shown in the flow chart below in Figure 4.

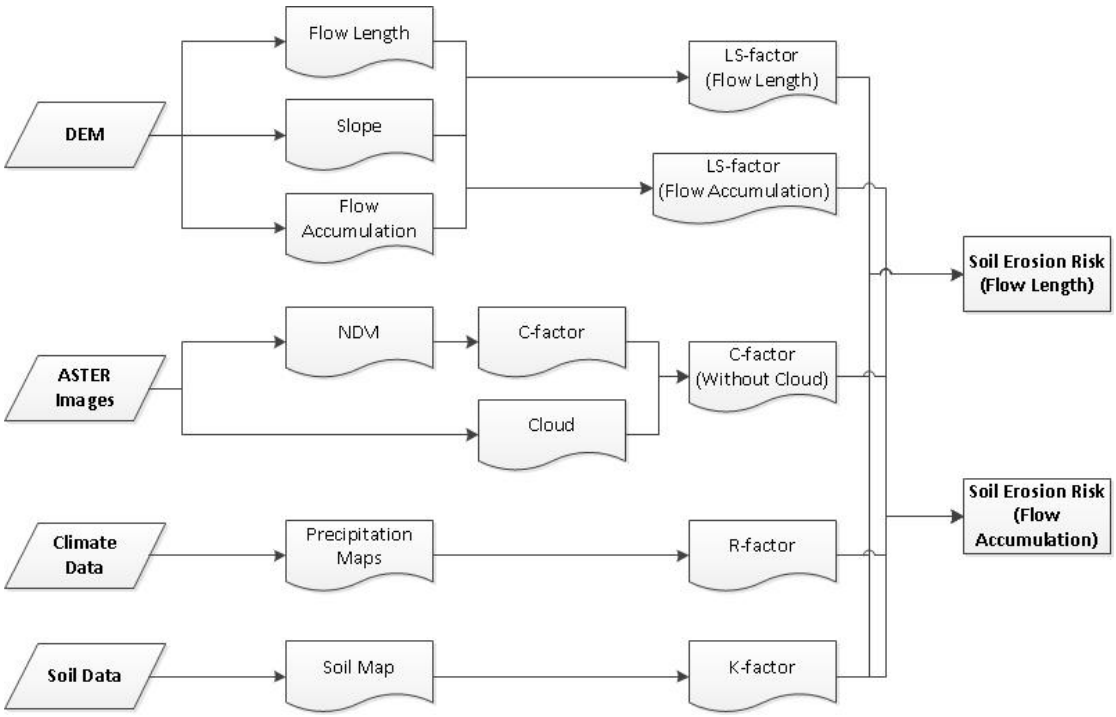

Figure 4. Flow chart of RUSLE modeling.

4.2 Rainfall erosivity factor (R)

The rainfall erosivity factor indicates the erosive force of a specific rainfall (Prasannakumar et al., 2012). The relationship between rainfall erosivity and rainfall depth developed by Wischmeier & Smith (1978) and modified by Arnoldus (1980) was used to translate the rainfall depth to rainfall erosivity. The calculation formula was as follows:

$$R = \sum_{i=1}^{12} 1.735 \times 10^{(1.5 \times \log_{10}(\frac{P_i^2}{P}) - 0.08188)} \quad (2)$$

where R is rainfall erosivity value in MJ mm ha^{-1} $h^{-1}y^{-1}$, Pi is the monthly rainfall in mm; and P is the annual rainfall in mm.

In order to apply the relationship above, the monthly and annual rainfall depth are required to be prepared in raster format. Thus, the original rainfall data which distributed in daily form from four climate stations was extracted and summed up to monthly rainfall and annual rainfall depth for the three target year 2000, 2006 and 2012. The position of the stations and the corresponding rainfall depth values were imported to ArcGIS as point vector data. Afterwards, Inverse Distance Weighting (IDW) interpolation with second power calculation was applied to create totally 13

rainfall depth maps, 12 monthly and an annual rainfall depth maps, for each of the target years. The relationship developed by Wischmeier & Smith (1978) was used to construct rainfall erosivity maps.

As the results of the relationship, the rainfall erosivity of the study area for the year 2000, 2006 and 2012 varies from 897 to 2813 MJ mm ha^{-1} $h^{-1}y^{-1}$. The highest and lowest values both appear in the year 2000. The southwestern part of the study area always has the highest rainfall erosivity values. Three rainfall erosivity maps are using the same stretch method and stretch scale to help comparison.

In Figure 5 below, the spatial distribution of the computed rainfall erosivity for the year 2000 is given. The range of the rainfall erosivity varied from 897 to 2813 MJ mm ha^{-1} $h^{-1}y^{-1}$ with the average value 1448 MJ mm ha^{-1} $h^{-1}y^{-1}$.

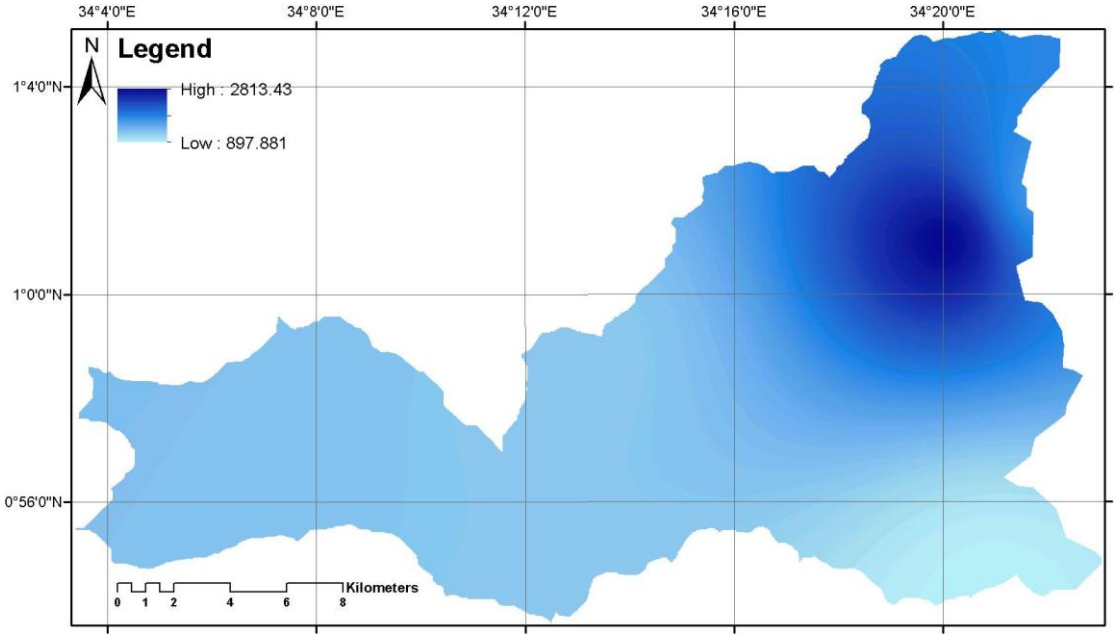

Figure 5. Rainfall erosivity map for the year 2000.

For the year 2006, the rainfall erosivity factor was found to be 1027 to 1607 MJ mm ha^{-1} $h^{-1}y^{-1}$ with the average value 1200 MJ mm ha^{-1} $h^{-1}y^{-1}$ for the entire study area. The map showing rainfall erosivity factor is shown in Figure 6.

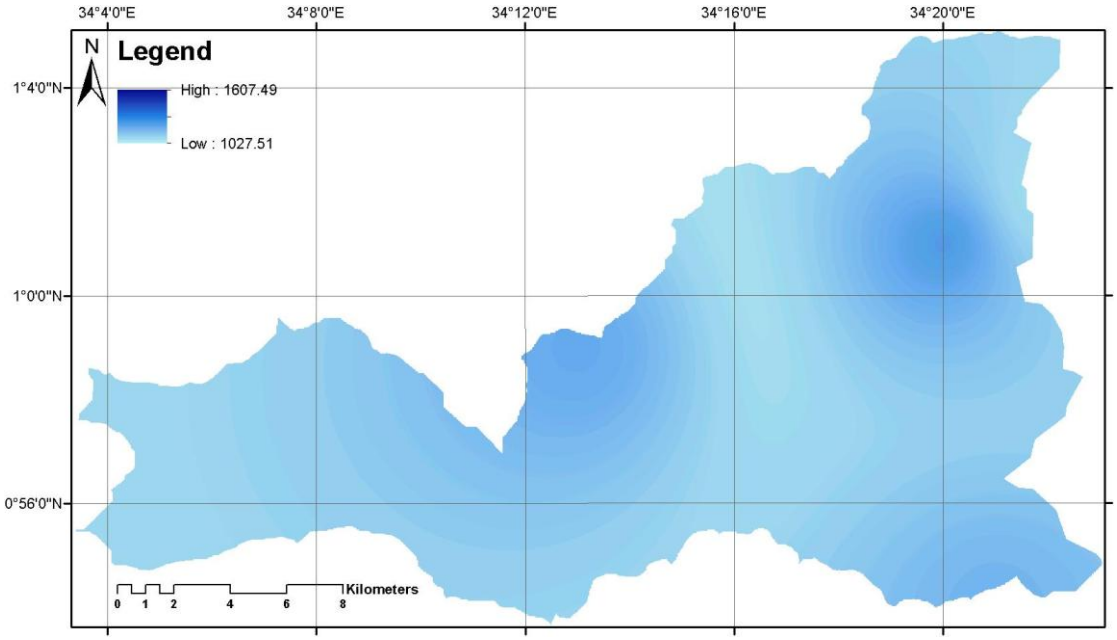

Figure 6. Rainfall erosivity map for the year 2006.

From the rainfall erosivity map Figure 7 for 2012, the largest amount of rainfall was observed. The map shows the range of the factor values changed from 1249 to 2803 MJ mm ha^{-1} $h^{-1}y^{-1}$ with the highest average value 1776 MJ mm ha^{-1} $h^{-1}y^{-1}$ in the three target year.

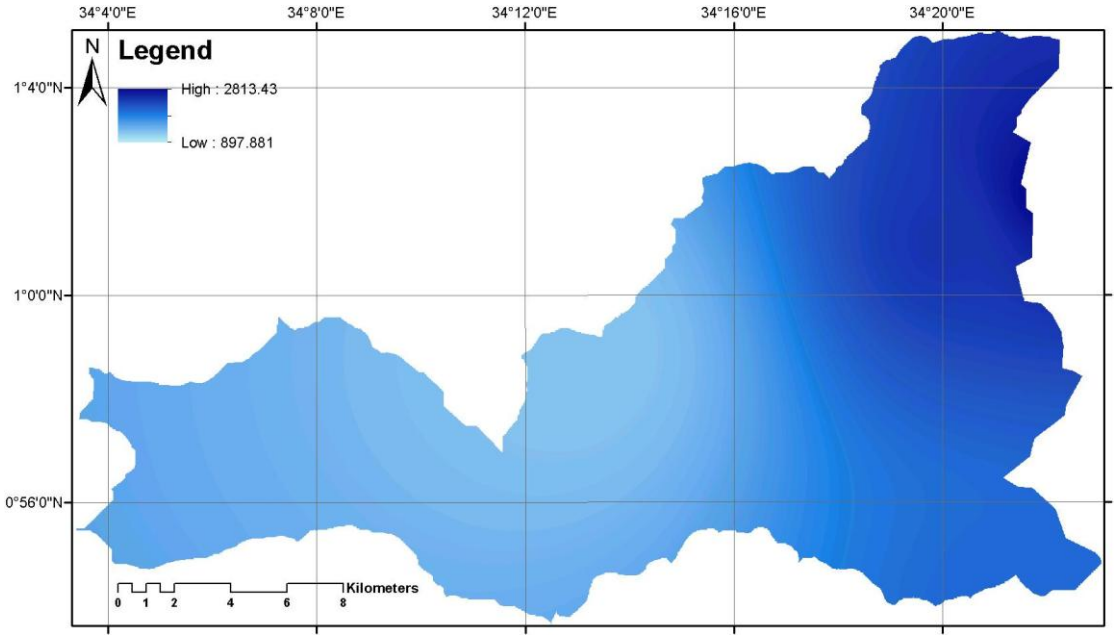

Figure 7. Rainfall erosivity map for the year 2012.

4.3 Soil erodability factor (K)

Soil erodability values were estimated based on the soil map, which contains the soil classification according to FAO standards. The finial soil map is shown below in Figure 8. There are totally five types of soil classified in the study area, Nitisols, Gleysols, Petric Plinthols (Acric), Lixic Ferralsols and Acric Ferralsols.

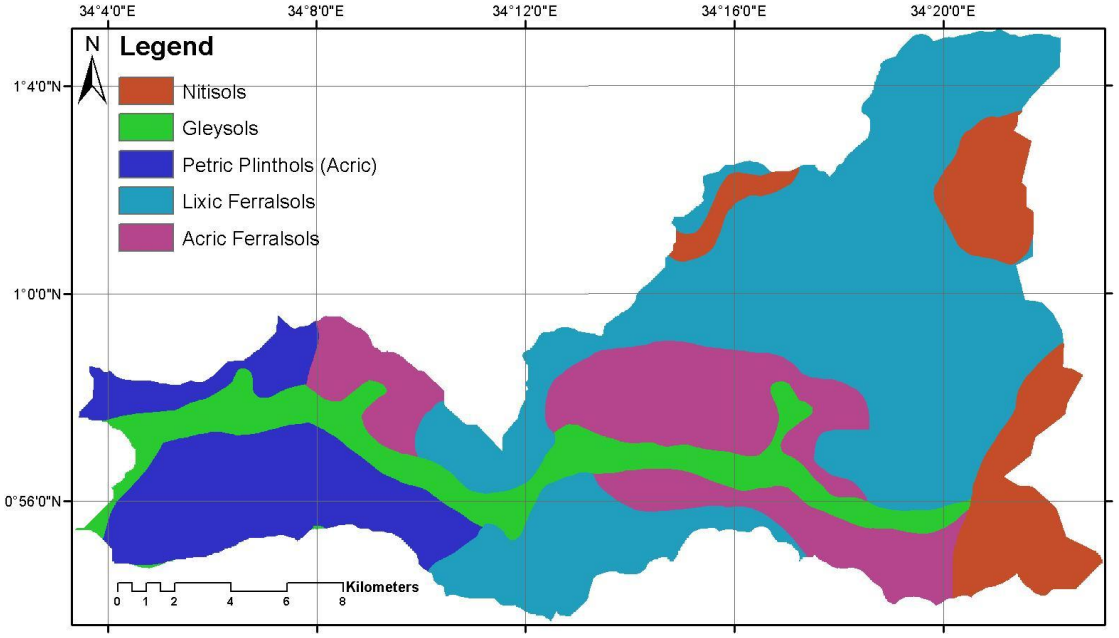

Figure 8. Soil map contains five different soil types in the study area.

Table 3 presents the percentage of the area taken by each type of soil. Lixic Ferralsols takes 46.6% of the study area. The other four types of soil take the area from 10% to 20 %.

Table 3. The percentage of the area taken by five types of soil.

Soil Types	Percentage of Area (%)
Nitisols	10.8
Gleysols	10.9
Petric Plinthols (Acric)	14.0
Lixic Ferralsols	46.6
Acric Ferralsols	17.7

Different soil types normally have different structure, which influence the intensity of the soil erosion. The soil erodability K-value indicates the vulnerability and susceptibility of the certain type of soil to detachment by erosion (Hoyos, 2005). The higher erodibility value the soil has, the more erosion will be suffered when the soils are exposed to the same intensity of rainfall, splash or surface flow (Hudson, 1981). The unit for soil erodibility is t ha h ha^{-1} MJ^{-1} mm^{-1}.

Pilesjö (1992) estimates soil erodibility values using the color of the soils according to Bono & Seiler (1983), Bono & Seiler (1984) and Weigel (1985). There are some other professional calculation methods for K-value, but more detailed information is required for different types of soil. In this case, this is the best way the estimated K-value due to the limitations from available data. Table 4 below shows the K-value for different soil colors.

Table 4. The K-value for different soil color.

Color	K-value
Black	0.15
Brown	0.2
Red	0.25
Yellow	0.3

The five different soil types were assigned K-values according to the color of the soils. The colors for the five different types of soil are obtained from ISRIC (World Soil Information) (2013). For the Ferralsols soil, there is no detailed subclass classification in the ISRIC document. The color is set to either red or yellow. The K-values for these two Ferrosols were thus set using the mean K-value of red and yellow color. The K-values of the five types of soil are shown in Table 5.

Table 5. The colors and corresponding K-values for soils in the study area.

Soil Type	Color	K-value
Nitisols	Red	0.25
Gleysols	Black	0.15
Petric Plinthols (Acric)	Red	0.25
Lixic Ferralsols	Red or Yellow	0.275
Acric Ferralsols	Red or Yellow	0.275

With the help of reclassification tool in ArcGIS, the cell values which indicated the soil types were replaced by using the K-values shown above. Three different K-values are obtained finally, 0.15, 0.25, 0.275 $\mathrm{t\,ha\,h\,ha^{-1}\,MJ^{-1}\,mm^{-1}}$. The map of soil erodability factor is shown in Figure 9.

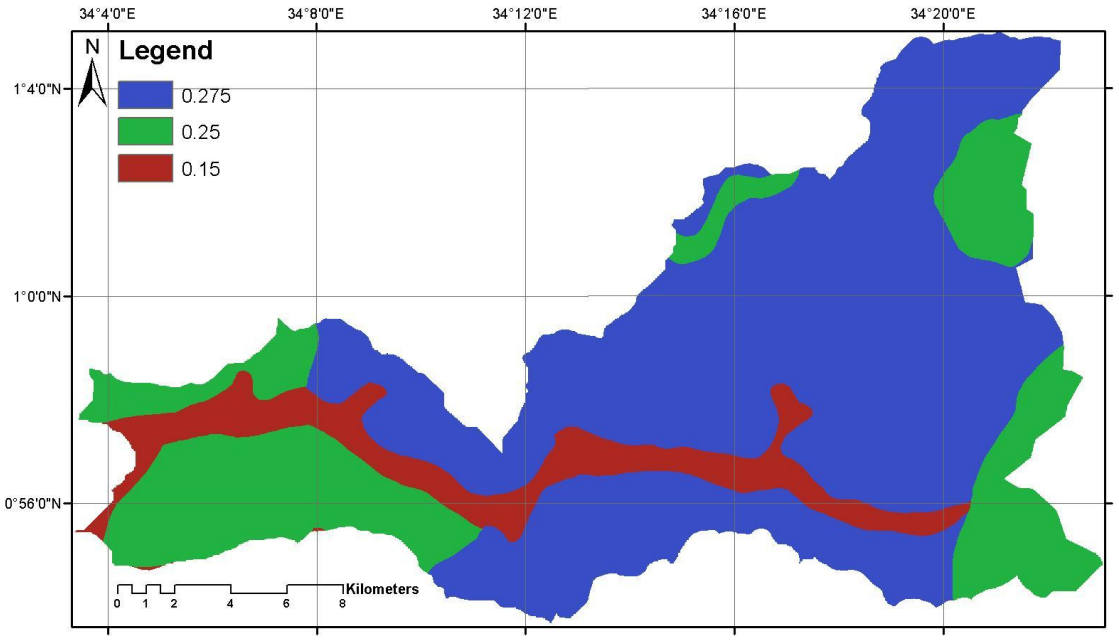

Figure 9. The translated soil erodability (K-value) factor map of the study area.

4.4 Slope length and steepness factor (LS)

The slope and steepness factor (LS) is a combination of slope steepness and slope length, to high degree affecting the total sediment yield from site. It is considered to be one of the most challenging to derive (Fu et al., 2005). Prasannakumar et al. (2012) claim that generating the LS-factor also captures factors like compaction, consolidation and disturbance of the soil.

In this study, two different parameters are used to calculate the LS-factor, flow length and flow accumulation. With the help of ArcGIS, the original DEM with 25 meters resolution was firstly converted to slope map in degree and flow direction map. Afterwards, the flow direction map was used to create maps of flow length and flow accumulation. According to the smallest pixel size from satellite images, maps of flow length and flow accumulation were resampled to 15 meters resolution.

Both flow length and flow accumulation can be used to estimate the contribution of upstream cells in a DEM to the downstream cells. Flow length, also called slope length, estimates the water flow along lines while flow accumulation is based on drainage area. For a specific cell, the flow accumulation is estimated based on the upslope area and not just along flow lines.

The LS factors were estimated applying the equation proposed by Moore & Burch (1986a, b). In the equation, the flow length and flow accumulation part is the number

of upslope cells which contribute to a given cell. In addition, in ArcGIS calculation, both flow length and flow accumulation are the number of upslope cells which contribute to a particular cell, so they can be replaced by each other in the equation. The relationship is as follows:

$$LS = (\text{Flow length (or Flow accumulation)} \times \frac{\text{Cell size}}{22.13})^{0.4} \times ((\sin \text{slope})/0.0896)^{1.3} \quad (3)$$

where LS is the combination of slope length and steepness; Flow accumulation or flow length is the accumulated upslope contribution to a cell; Cell size is the resolution of the raster image, and Sin slope is the sin value of the slope in degrees.

The estimated LS values based on flow length, varying between 0 and 184, are presented in Figure 10.

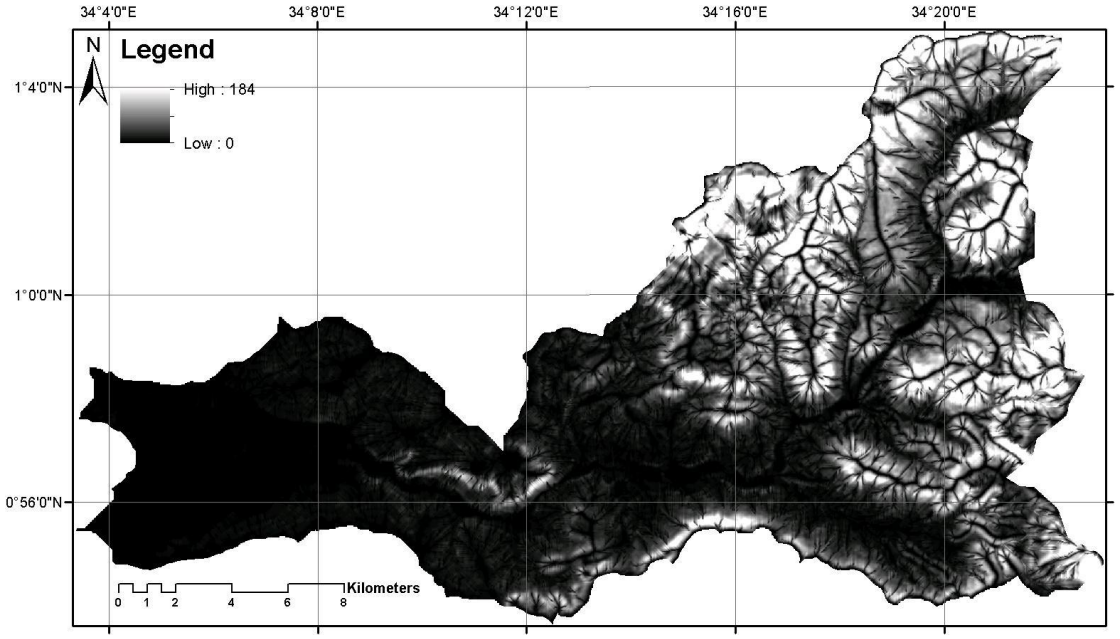

Figure 10. LS-factor map obtained by using flow length.

For the second method, flow accumulation was used in the formula to replace the variable flow length. LS-factor map looks like the map below in Figure 11. It is very similar to the LS-factor map obtained by using flow length, but the range of the values varies from 0 to 95.

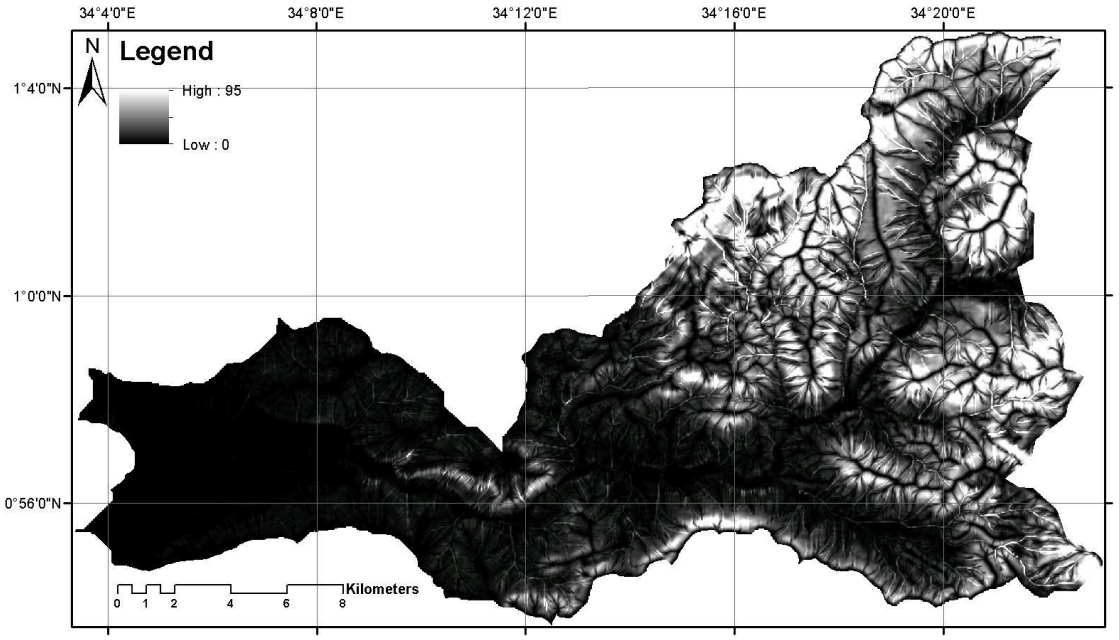

Figure 11. LS-factor map obtained by using flow accumulation.

4.5 Cover management factor (C)

The cover management factor represents the effect of plants, crop sequence and other cover surface on soil erosion. The value of C-factor is defined as the ratio of soil loss from a certain kinds of land surface cover conditions (Wischmeier & Smith, 1978).

According to Prasannakumar et al. (2012), the Normalized Difference Vegetation Index (NDVI) can be used as an indicator of the land vegetation vigor and health. In addition, Karydas et al. (2009) and Tian et al. (2009) state that due to the variety of the land cover patterns, satellite remote sensing data can act as an extremely important role to estimate the C-factor.

In this study, the original satellite images from the year 2000, 2006 and 2012 with the reflectance values in bands green, red and near-infrared, were converted to NDVI for the corresponding years. The NDVI calculation formula can be represented as following:

$$\mathrm{NDVI} = \frac{\mathrm{rNIR} - \mathrm{rRed}}{\mathrm{rNIR} + \mathrm{rRed}} \tag{4}$$

where rNIR is the reflectance value in near-infrared band; rRed is the reflectance value in visible red band.

After calculated NDVI, the C-factor can be estimated by applying the relationship used in Zhou et al. (2008) and Kouli et al. (2009):

$$C = \exp\left(-\alpha \times \frac{NDVI}{\beta - NDVI}\right) \quad (5)$$

where C is the calculated cover management factor; NDVI is the vegetation index, and α and β are two scaling factors. Van der Knijff et al. (2000) suggest that by applying this relationship, better results than using a linear relationship can be obtained. They suggest the values for the two scaling factors α and β to be 2 and 1, respectively.

Because of the cloud cover in the rainy season, the quality of the satellite images is limited, which may cause some uncertainties in the results. In order to remove cloudy areas, the clouds and the shadow of clouds, were classified by using unsupervised classification with the spectral bands green, red and near-infrared. The number of unsupervised classes was set to 15 classes. The classes, automatically clustered by the unsupervised classification tool in ArcGIS, were finally grouped to construct cloud layers. In the C-factor maps and final results, the clouds areas are shown as the black with no data. Figure 12 shows the coverage percentage of classified cloud in the study area.

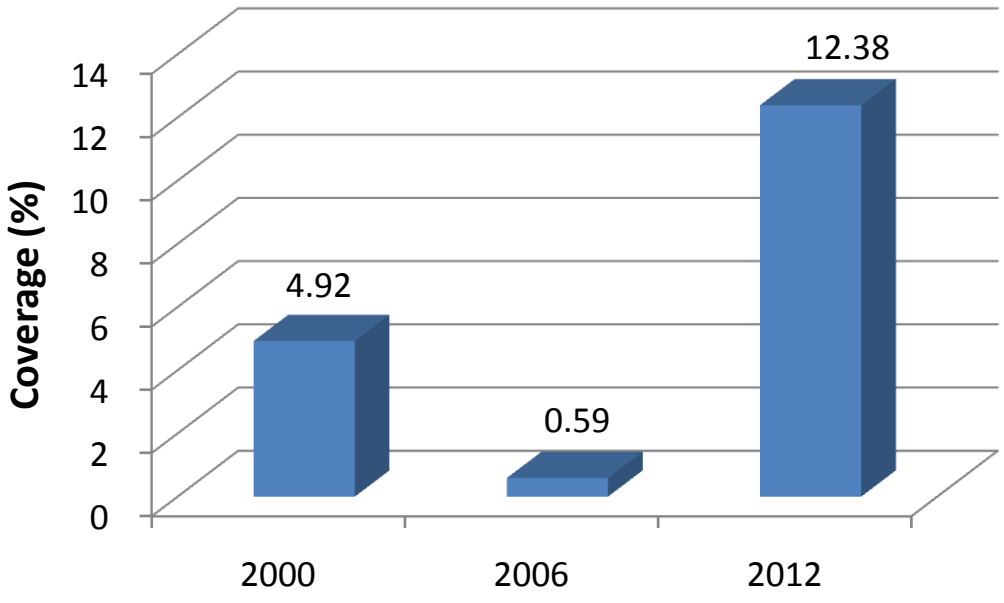

Figure 12. Coverage percentage of the classified cloud in the study area.

Obviously, in the year 2012, 12.38% of the study area is covered by clouds. And only 0.59% of the study area, which is the least, is covered by clouds in the year 2006. For

cloud problem, more explanation and discussion is handed out in discussion section. In the last step to generate C-factor maps, a low pass filter was applied to smooth the images, in order to decrease the negative influence of the noise in satellite data. At the same time, some uncertainties were caused because of the filter.

By running the formula with the raster calculator tool in ArcGIS, the C-factor maps were obtained. For the year 2000, C-factor values varied from 0.00008 to 0.58 and the spatial variability is shown in Figure 13. According to the map, some clouds are located along the east boundary of the study area.

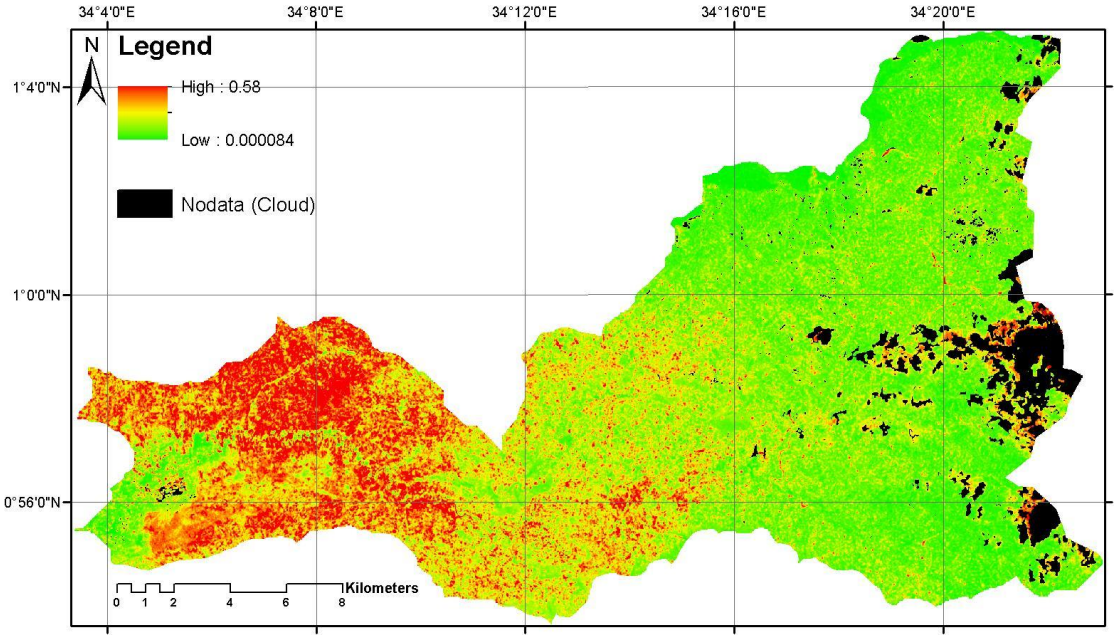

Figure 13. C-factor map of the study area in the year 2000.

For the year 2006, the C-factor map is shown in Figure 14. The C-factor varies from 0.0002 to 0.66. This image contains the least clouds among the three C-factor maps for the target years. Therefore, it may have the least uncertainties caused by cloud cover.

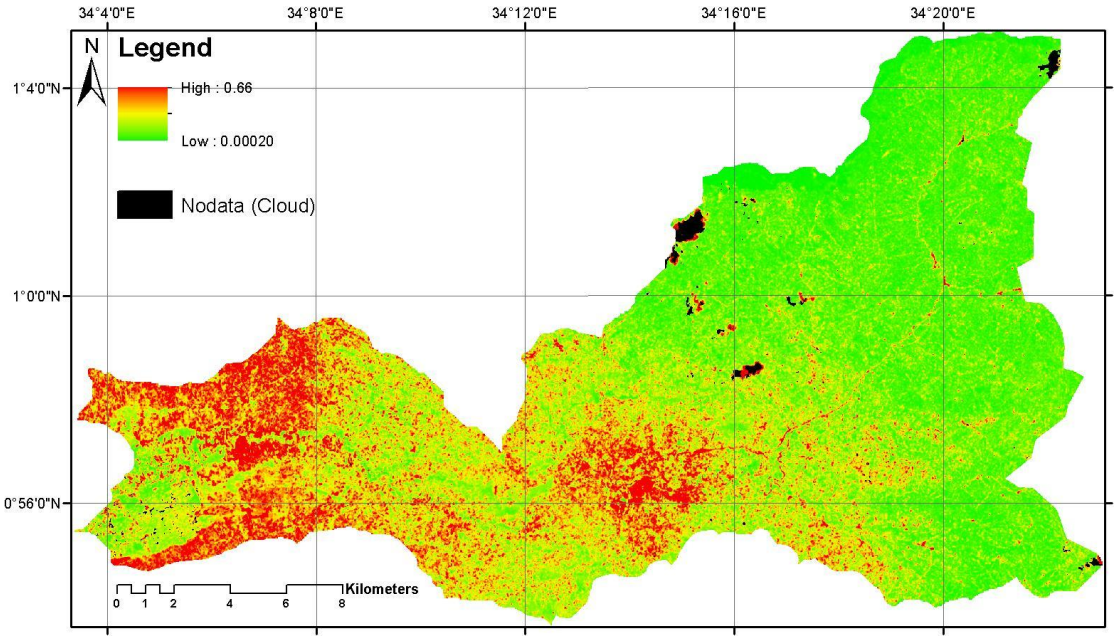

Figure 14. C-factor map of the study area in the year 2006.

With the map showing the C-factor for the year 2012 presented below in Figure 15, the C-factor values vary from 0.0027 to 0.55. For the year 2012, the satellite image is covered by clouds with 20%. Therefore, in the result map of C-factor, the cloud area which is shown as no data is the most among the three C-factor maps.

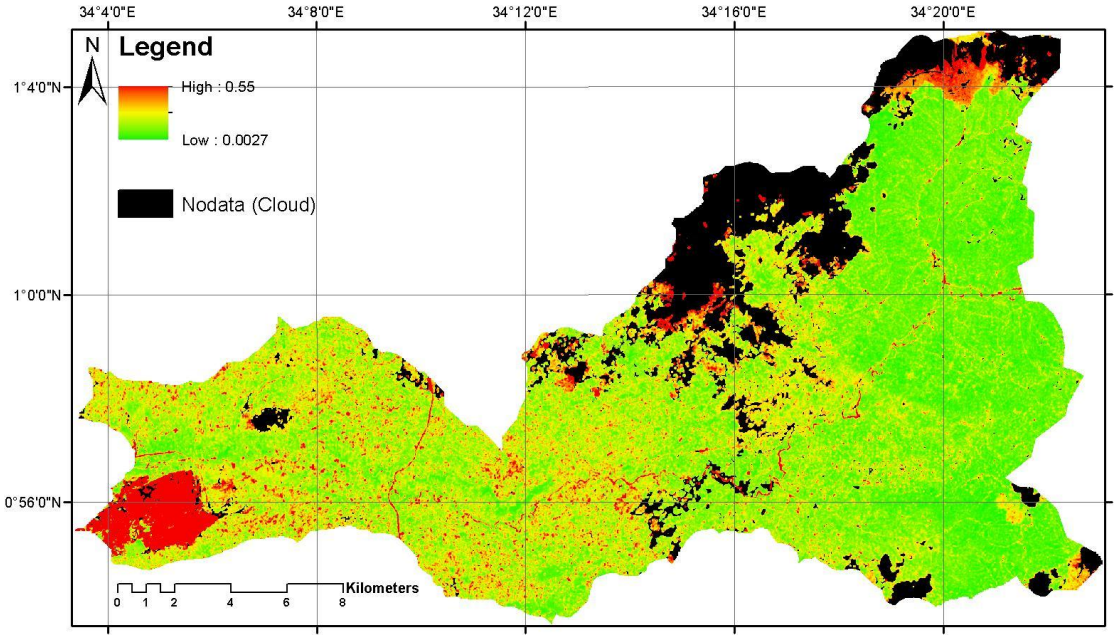

Figure 15. C-factor map of the study area in the year 2012.

As presented in the three C-factor maps (Figures 13, 14, 15), it is obvious that the areas around or close to the clouds has very high C-factor values, which are shown in reddish color. These areas are the shadows of the clouds. This issue will cause some uncertainties. The detailed explanation is given in the discussion section.

4.6 Conservation practice factor (P)

The conservation practice factor (P) is also called as support factor. It represets the soil-loss ratio after performing a specific support practice to the corresponding soil loss, which can be treated as the factor to represent the effect of soil and water conservation practices (Omuto, 2008; Renard et al., 1997). The range of P factor varies from 0 to 1. The lower the value is the more effective the conservation practices are.

In this study, this conservation practice factor was assigned to the maximum value of one (1) for the entire study area for running the RUSLE model. It is because there are no significant conservation practices detected. In Manafwa, most of the conservation practices are tree planting, and can thus be considered to influence the cover management factor (C) (Bamutaze, 2010).

5. Results and Discussion

In order to estimate annual soil loss, the five factors were multiplied according to the relationship in RUSLE model. In total six layers with annual soil loss were computed, two for each year, one using flow length and one using flow accumulation. The soil loss was classified into soil erosion risk maps with five different soil erosion risk levels according to Bamutaze (2010). The threshold for each of the risk level is presented in Table 6.

Table 6. Categorization of soil erosion risk.

Erosion Risk	**Threshold (t ha^{-1} y^{-1})**
Very Low	Soil Loss $\leqslant 2$
Low	$2 <$ Soil Loss $\leqslant 10$
Moderate	$10 <$ Soil Loss $\leqslant 50$
High	$50 <$ Soil Loss $\leqslant 100$
Very High	Soil Loss $\geqslant 100$

5.1 Soil erosion risk based on flow length method

In general, the soil erosion risk maps obtained by flow length method have relatively high annual soil loss values. Exploring the maps (see Figure 16), it can be concluded that more than 50% of the area is exposed for very high erosion risk.

For the year 2000, Figure 16 below illustrates the estimated erosion risk. The soil loss estimated by flow length method in this year varies between 0 and 4995 t ha^{-1} y^{-1}, with the average value 364 t ha^{-1} y^{-1}. The following histogram Figure 17 shows the land coverage percentage of each soil erosion risk level. 62.24% of the area has a very high erosion risk, 12.42% a high risk, 16.91% a moderate risk, 6.02% a low risk, and only 2.42% a very low risk of soil erosion.

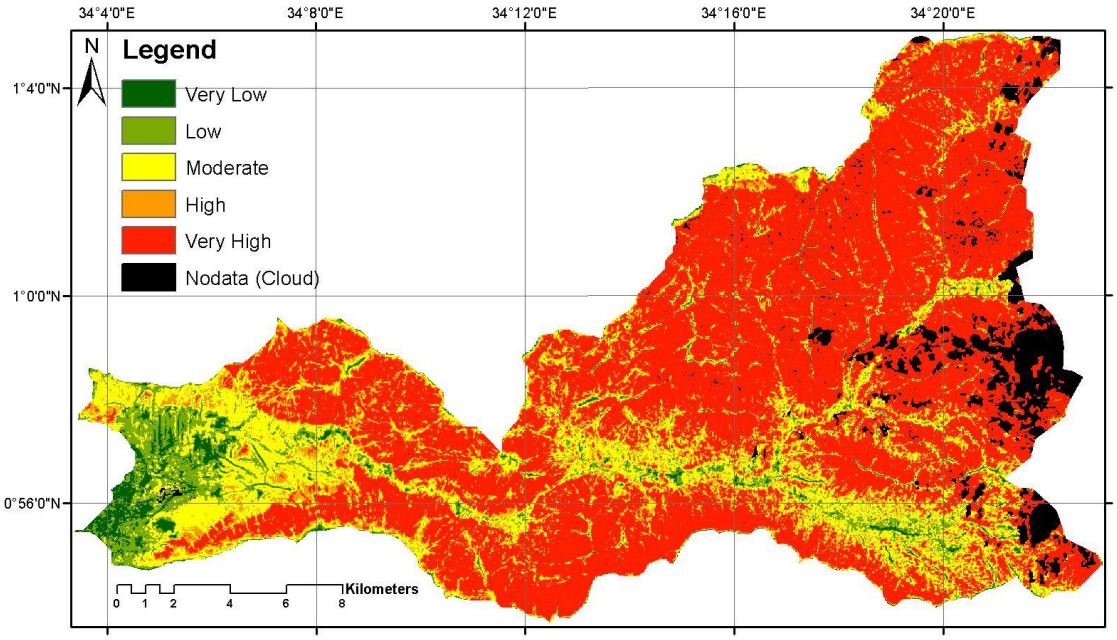

Figure 16. Soil erosion risk map obtained by flow length method for the year 2000.

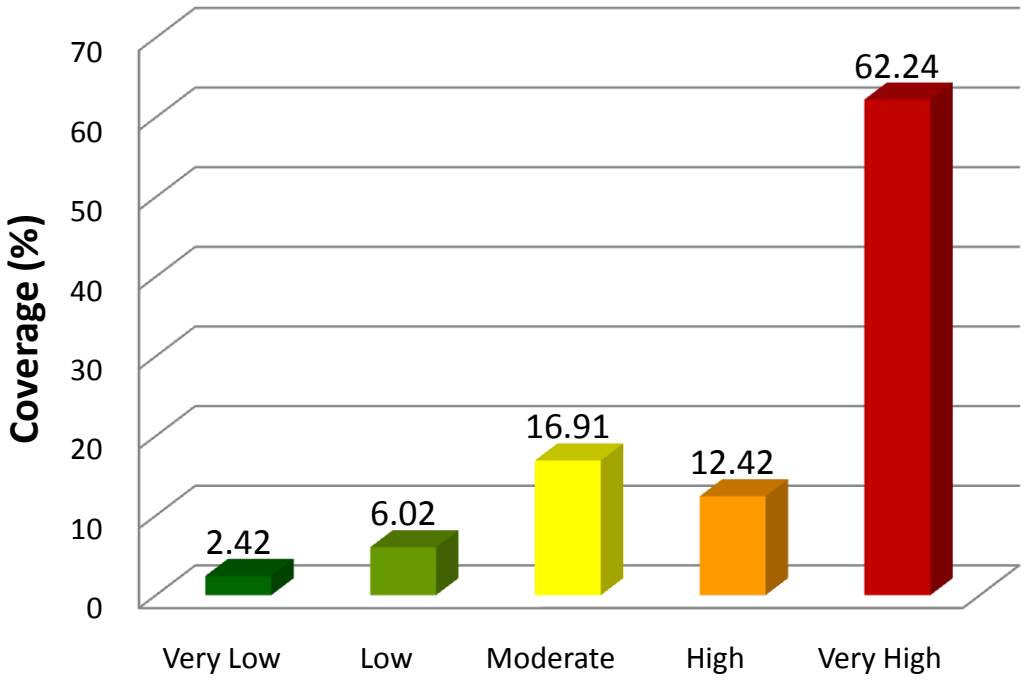

Figure 17. The percentage of coverage for the erosion risk map 2000 by flow length method.

For the year 2006, the erosion risk map is shown in Figure 18. The estimated annual soil loss varies between 0 and 4698 t ha^{-1} y^{-1}, which is similar to the result of year 2000. However, the mean value is 231 t ha^{-1} y^{-1}, which is much lower than 2000. The histogram Figure 19 shows that, 54.77% of the area has a very high erosion risk,

16.33% a high risk, 19.7% a moderate risk, 6.8% a low risk, and only 2.41% a very low risk of soil erosion.

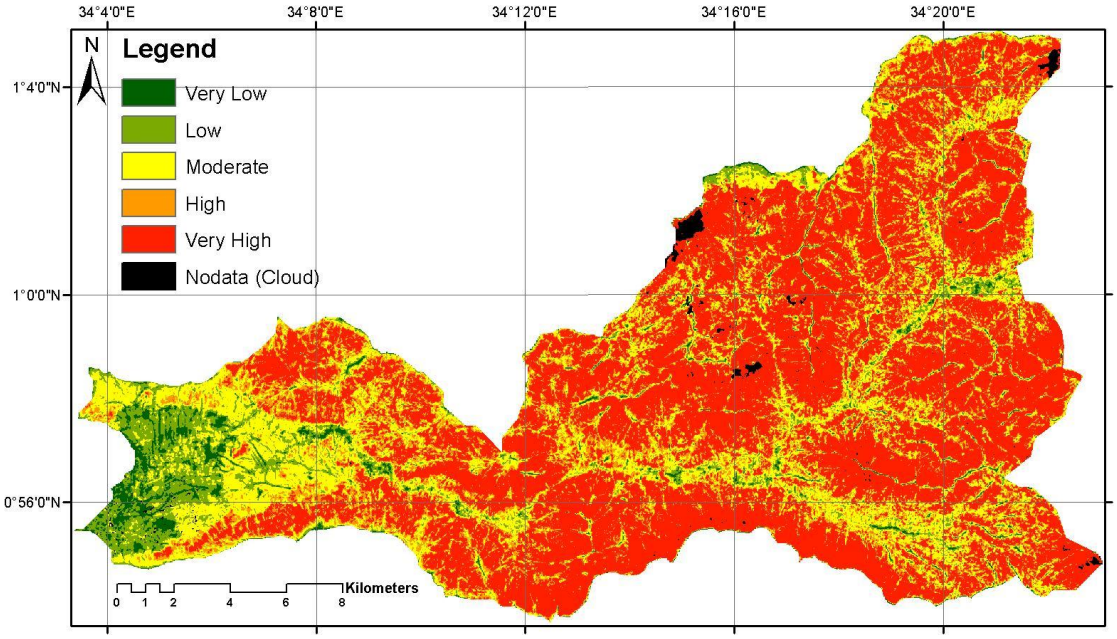

Figure 18. Soil erosion risk map obtained by flow length method for the year 2006.

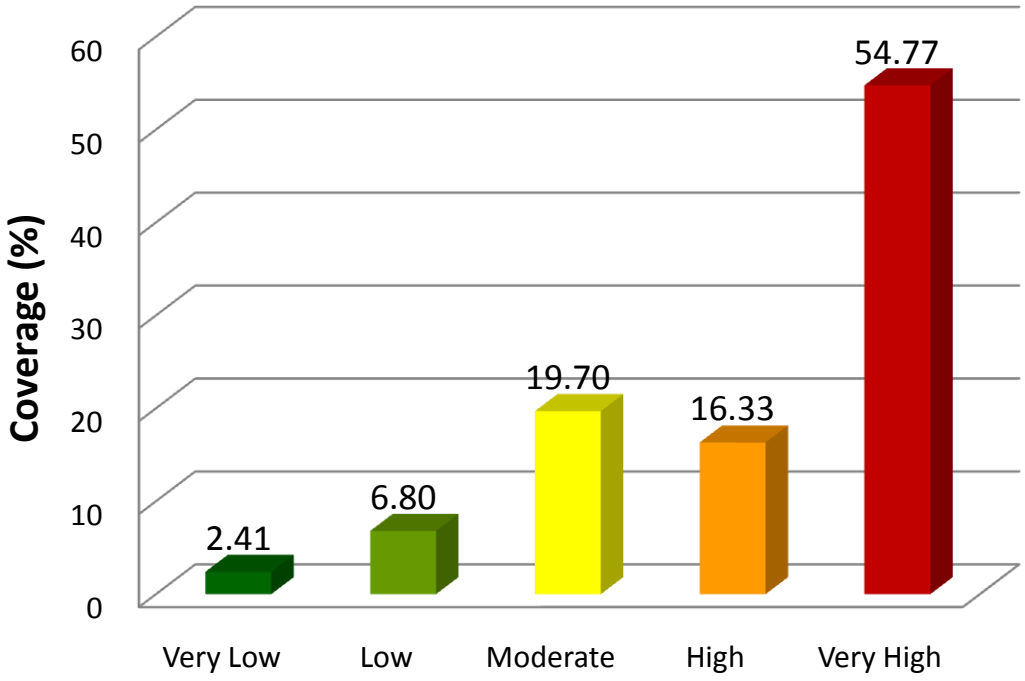

Figure 19. The percentage of coverage for the erosion risk map 2006 by flow length method.

The result for 2012 showed in Figure 20, the estimated soil loss values vary between 0 and 6053 t ha^{-1} y^{-1}. The mean soil loss value is 362 t ha^{-1} y^{-1}, which close to the one for year 2000. From the histogram Figure 21, 55.82% area is under very high

erosion risk, which closes to the year 2000. 55.86% of the area has a very high erosion risk, 14.23% a high risk, 19.8% a moderate risk, 7.45% a low risk, and only 2.69% a very low risk of soil erosion. There is a increasing for the area of low and moderate erosion risk compared with year 2000. The coverage percentage of year 2012 is very similar to the situation in 2006.

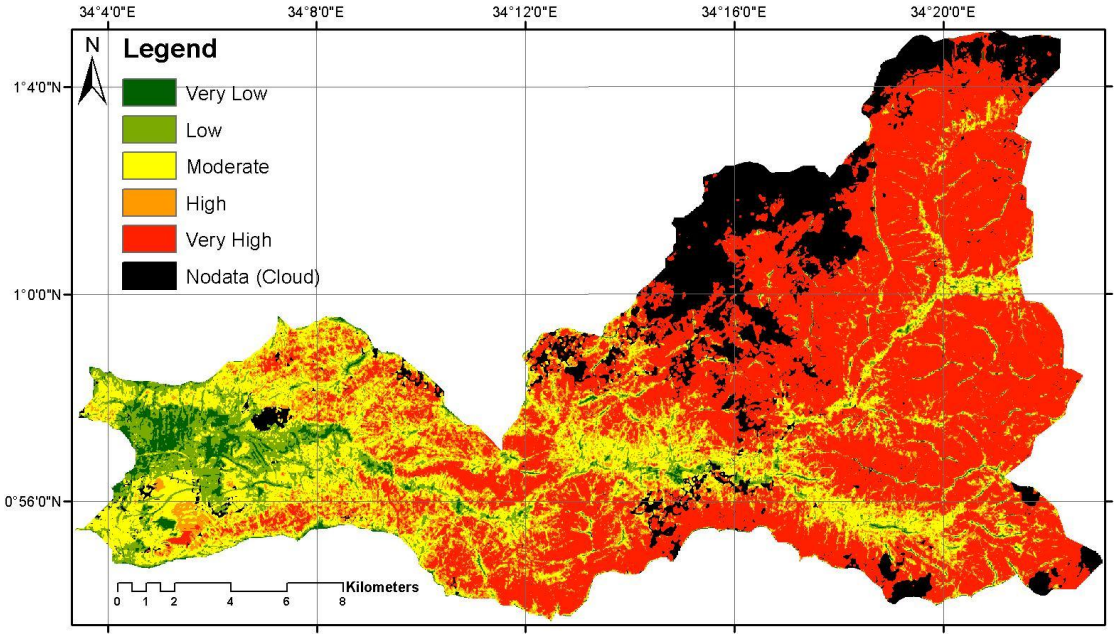

Figure 20. Soil erosion risk map obtained by flow length method for the year 2012.

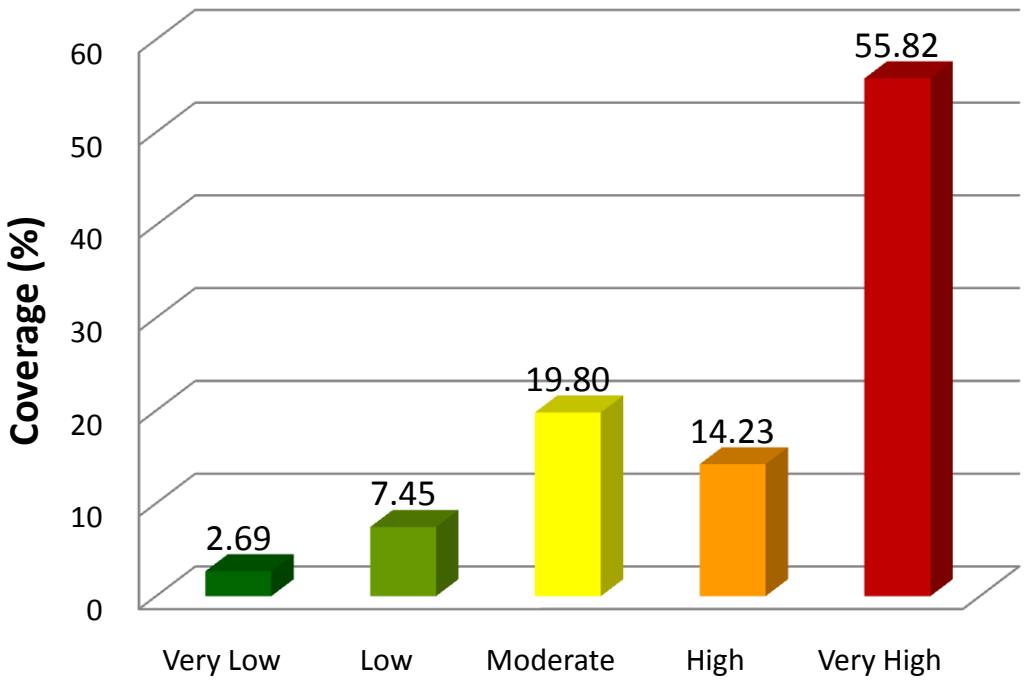

Figure 21. The percentage of coverage for the erosion risk map 2012 by flow length method.

5.2 Soil erosion risk based on flow accumulation method

Generally, the absolute values of annual soil loss using the flow accumulation are much smaller than the results estimated by using flow length method. The results also coincide better with field data, and thus more reliable.

In the year 2000, Figure 22 below, the highest estimated soil loss is 1198 t ha^{-1} y^{-1}. The mean value for the whole study area is 103 t ha^{-1} y^{-1}. In histogram Figure 23, 30.94% of the study area is classified to have a moderate soil erosion risk. Higher and much higher risks are allocated to 18.54% and 30.3% respectively, while 13.79% of the area has low erosion risk and 6.43% very low risk.

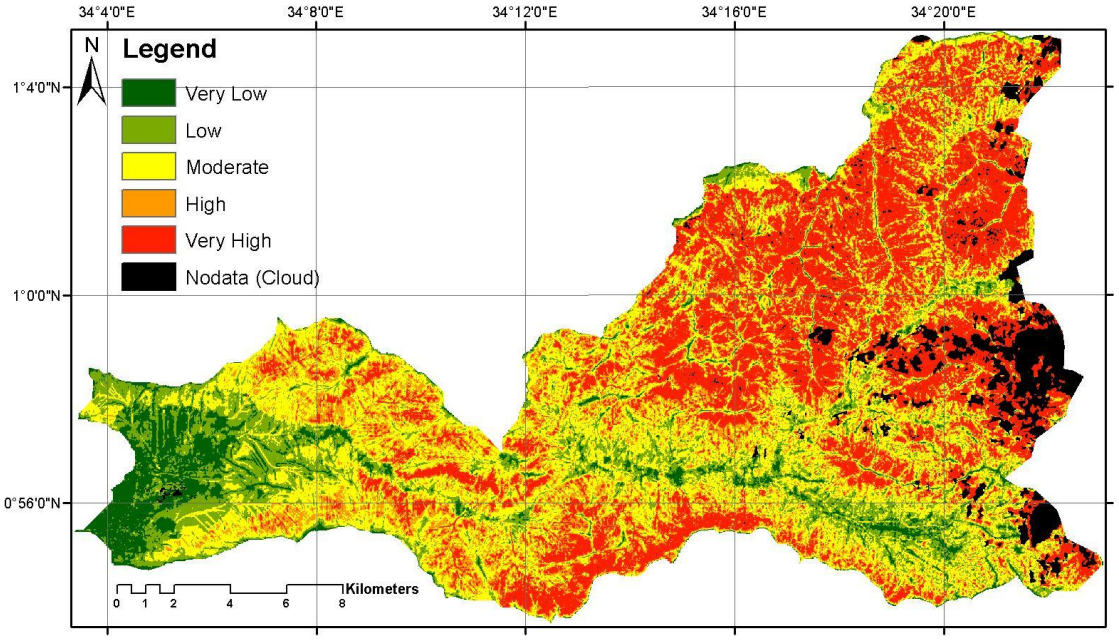

Figure 22. Soil erosion risk map obtained by flow accumulation method for the year 2000.

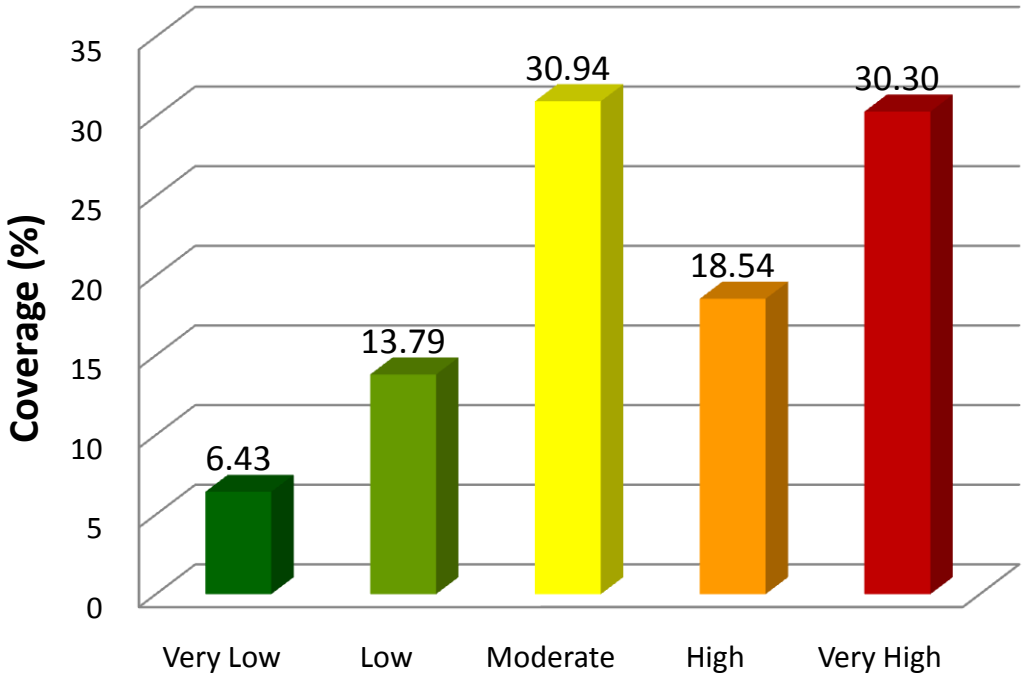

Figure 23. The coverage percentage of the erosion risk map 2000 by flow accumulation method.

The estimated soil erosion risk map for the year 2006 is shown in Figure 24. In this year, the estimated annual soil loss varies between 0 and 1129 t ha^{-1} y^{-1}, which is almost the same as for the year 2000. However, the mean value decreases to 67 t ha^{-1} y^{-1}, which is the lowest estimated mean soil loss value of all the results. From Figure 25, the histogram also shows that, 38.96% of the area has a moderate risk of soil erosion, high and very high risks are allocated to 19% each, 15.65% of the area has a low risk, and 7.05% has a very low risk of soil erosion.

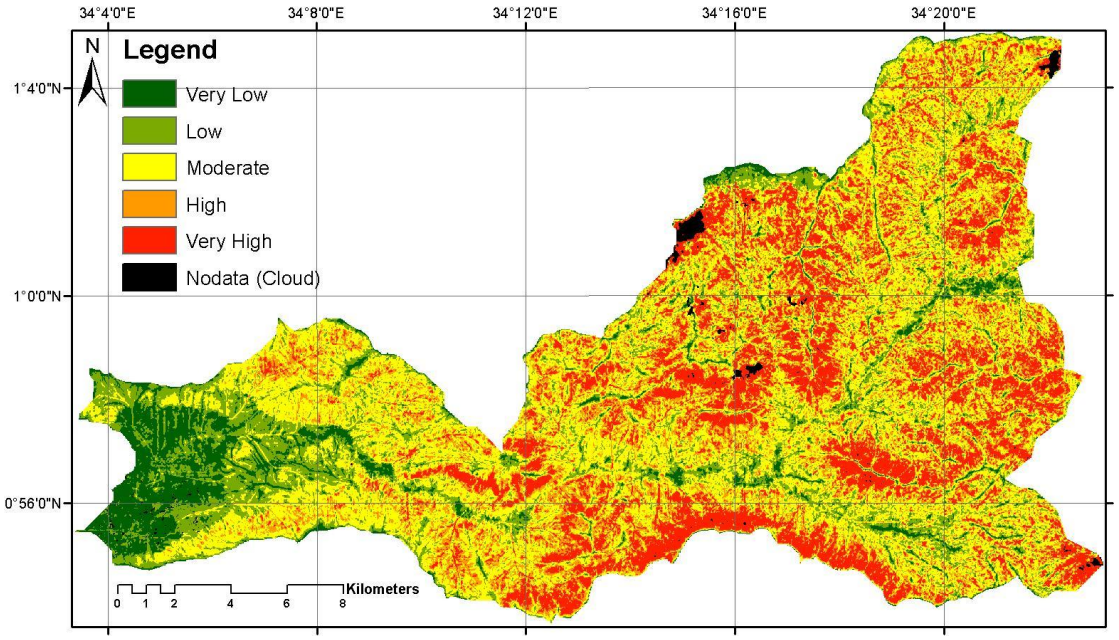

Figure 24. Soil erosion risk map obtained by flow accumulation method for the year 2006.

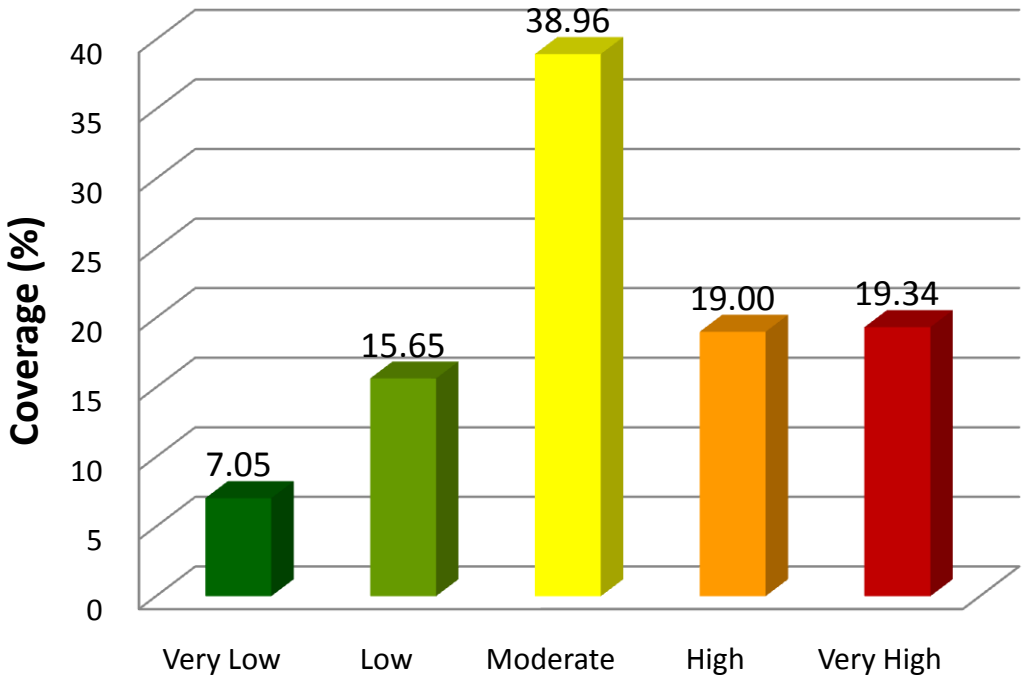

Figure 25. The coverage percentage of the erosion risk map 2006 by flow accumulation method.

For the erosion risk map Figure 26 in the year 2012, estimated soil loss varies between 0 and 1454 $\mathrm{t\,ha^{-1}\,y^{-1}}$. The value 1454 $\mathrm{t\,ha^{-1}\,y^{-1}}$ is higher than the maximum values for 2000 as well as 2006. As usual, the area covered by moderate

erosion risk is the most, which shows in the histogram Figure 27 with value 32.47%, followed by very high risk 27.85%, low and high risks 16%, and very low risk 7.84%.

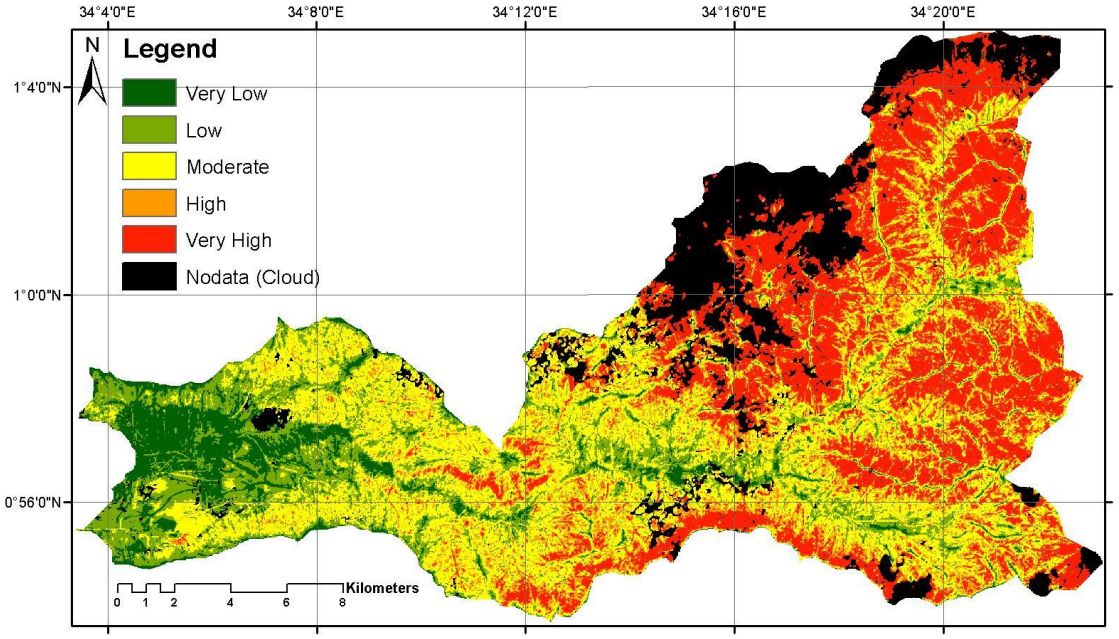

Figure 26. Soil erosion risk map obtained by flow accumulation method for the year 2012.

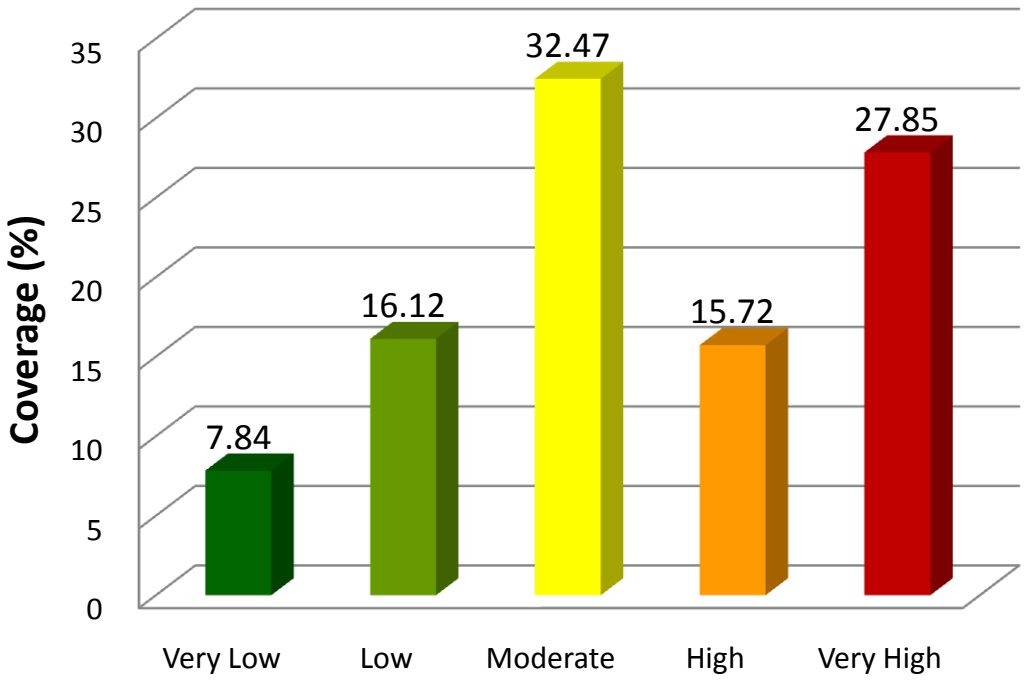

Figure 27. The coverage percentage of the erosion risk map 2012 by flow accumulation method.

5.3 Comparison of the two modeling methods

Based on the results obtained by the flow length and flow accumulation method, a comparison of accuracy was carried out in order to judge which of the two methods that gave the better and more accurate result. The comparison was made from two aspects.

Firstly, from the cartographic point of view, the estimated result maps obtained by using flow length method have a large area assigned high and very high soil erosion risk levels. The areas with very high erosion risk level are 62.24%, and 54.77% and 55.82% for the year 2000, 2006 and 2012, respectively. Comparing with field visits and interviews with farmers this is unrealistic. Additionally, the classification method used to generate the soil erosion risk maps is referring to a published study by Bamutaze (2010), reporting lower soil erosion risks in the region. Altogether, this indicates that the results obtained by using the flow accumulation method are better.

Secondly, according to the results reported by Bamutaze (2010), from a nearby area in the nineties, the average annual soil loss value was 43 $t\,ha^{-1}\,y^{-1}$, with the maximum value 585 $t\,ha^{-1}\,y^{-1}$ on pixel level, and the highest potential value reaching 778 $t\,ha^{-1}\,y^{-1}$. In the study presented in this project, the results obtained by using the flow accumulation method give the average annual soil loss values 103 $t\,ha^{-1}\,y^{-1}$, 67 $t\,ha^{-1}\,y^{-1}$, and 101 $t\,ha^{-1}\,y^{-1}$, with the highest values 1198 $t\,ha^{-1}\,y^{-1}$, 1129 $t\,ha^{-1}\,y^{-1}$ and 1454 $t\,ha^{-1}\,y^{-1}$ for the year 2000, 2006 and 2012, respectively. These estimates are much closer to the previous study than the results obtained by using the flow length method.

To conclude, the results obtained by using the flow accumulation method seem more accurate and reliable than using flow length. Thus, further discussion about the soil erosion trend and the relationships between soil erosion and precipitation and land cover is based on the results obtained by the flow accumulation method.

5.4 Soil erosion trends related to precipitation and land cover changes

Mean annual precipitation and mean R-factor of the study area for three years are presented in Figure 28 as blue and red line, respectively. From 2000 to 2006, the mean annual precipitation decreases from 1290 mm to 1200 mm. Afterwards, the increase from 1200 mm to 1249 mm from the year 2006 to 2012. The mean annual precipitation for 2012 is approximately the same as for the year 2000. The R-factor

shows the similar trend. However, the mean R-factor value in the year 2012 is significantly higher than during the year 2000 (1776 MJ mm $ha^{-1}h^{-1}y^{-1}$ and 1448 MJ mm $ha^{-1}h^{-1}y^{-1}$). This means that the rainfall 2012 has the biggest effect on soil erosion among the three target years.

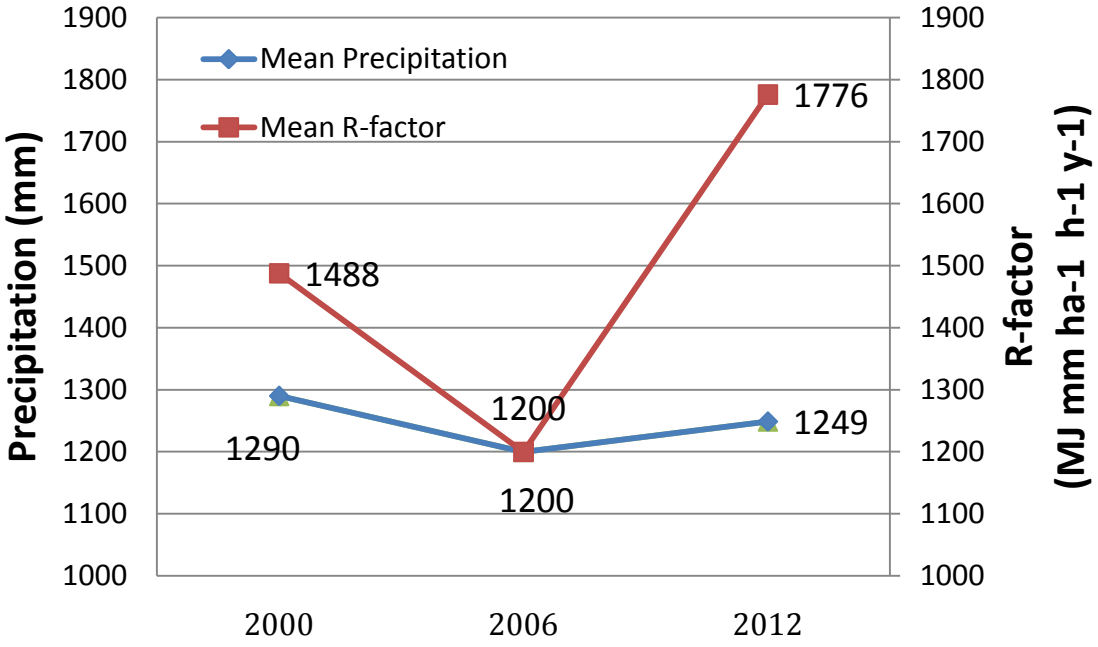

Figure 28. Precipitation and R-factor changes from 2000 to 2012.

Regarding land cove, mean NDVI was used as the detector for land cover changes. As illustrated in Figure 29, mean NDVI values increase from 0.56 to 0.59 during the years 2000 to 2012. The increasing trends considered as very weak.

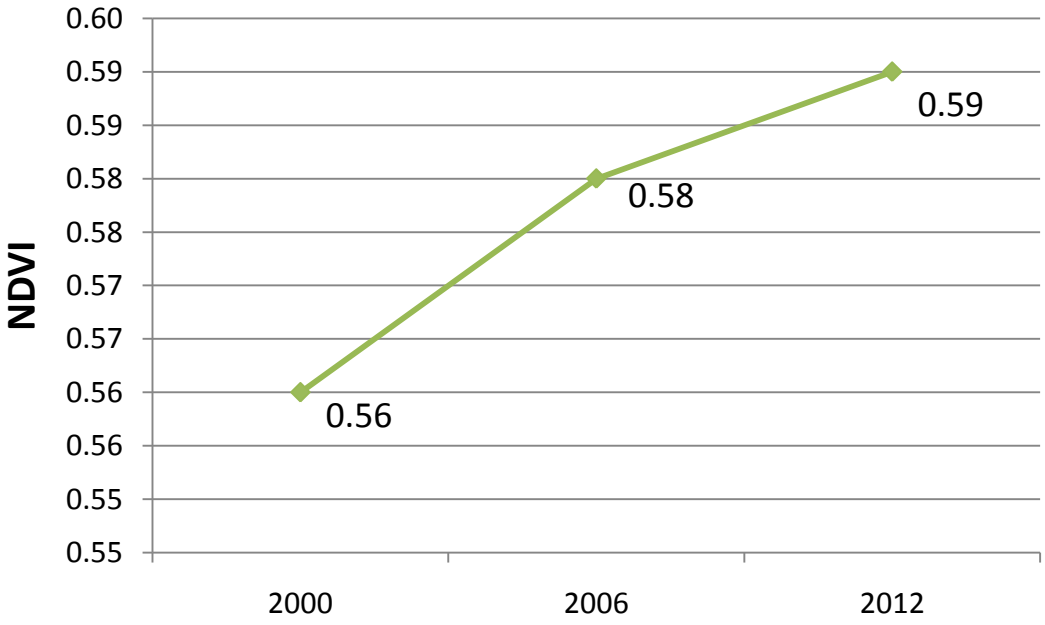

Figure 29. Mean NDVI for entire study area from year 2000 to 2012.

In more detailed, the histogram in Figure 30 shows comparison of the NDVI increase and decrease among the three target years. The increasing of NDVI indicates better ground cover vegetation condition. The maps showing NDVI changes among year 2000, 2006 and 2012 are located in Appendix Figure 1, 2 and 3.

From the year 2000 to 2006, 57.14% of the land area has an increasing NDVI. This area is mainly located in the western part of the study area. The area with decreasing (47%) appears mainly in the south and east. From 2006 to 2012, an increasing trend is kept with the increasing coverage percentage of 58.58%. The increasing NDVI is still located in the western part of the study area. The decreasing NDVI is mainly in the northeast. Comparing the year 2000 and 2012, 64.06% of the land has an increasing NDVI. Even if the analysis is influenced by cloud cover and not significant, one can see clear indications that most of the western part of the study area has got more vegetation cover during the last decade. However, a regular polygon located in the southwest corner has a large decrease in vegetation cover, may be caused by artificial activities such as urban construction, or agriculture land conversion.

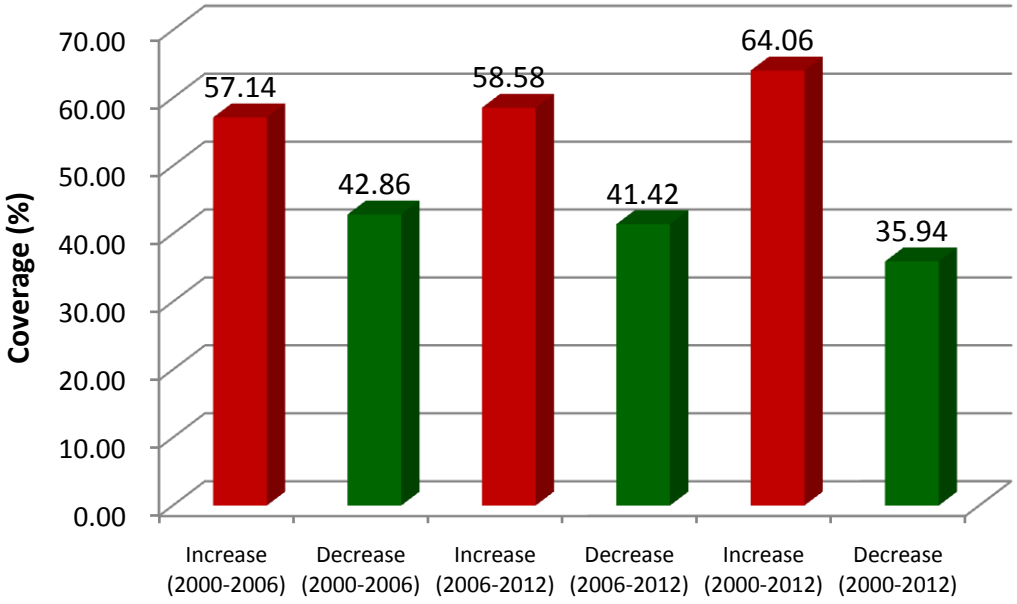

Figure 30. Coverage percentage of NDVI increase and decrease from year 2000 to 2012.

Soil erosion changes and trends can be explored in Figure 31 below. The estimated soil erosion decreases between 2000 and 2006, and increases between 2006 and 2012. This "trend" is similar to the precipitation trend discussed before. The R-factor in the year 2006 is much lower than the year 2000 and 2012 which is shown in Figure 28. It

seems that soil erosion is more sensitive to precipitation and to be no significant relationship between land cover changes and soil erosion on study area scale.

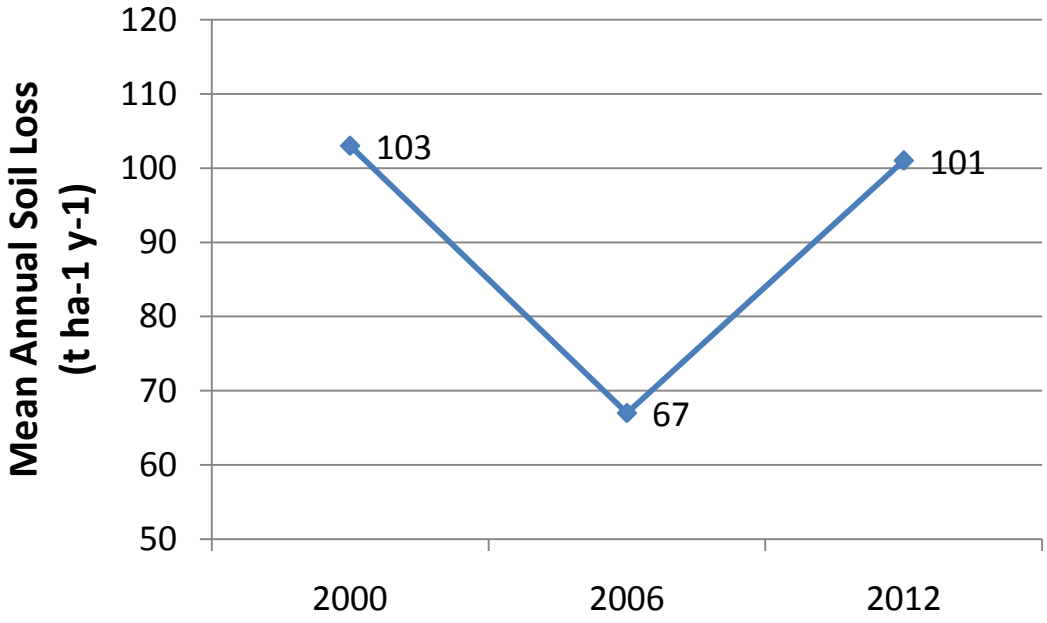

Figure 31. Mean annual soil loss for entire study area from year 2000 to 2012.

With illustration in Figure 32, the histogram indicates the increase and decrease of annual soil loss among the year 2000, 2006 and 2012. The maps presenting increase and decrease of annual soil loss is attached in Appendix Figure 4, 5 and 6. From year 2000 to 2006, 65.57% of the study area has a deceasing trend of annual soil loss. Most of the area with large decrease is located in the northeastern part of the study area. From 2006 to 2012, there is a general increase in soil erosion risk (52.17% of the study area). The areas with higher risk for soil erosion are generally located in the southwestern part of the study area. When comparing the two years 2000 and 2012, one can conclude that 60.51% of the land has a decreasing trend in soil erosion risk. The 39.49% of the land with an increasing risk is mainly located in northeastern corner, southeastern corner, and some of the western part of the study area. The relatively high decrease in soil erosion risk can be seen as contradictory in comparison with the high maximum soil loss (1454) detected in the year of 2012. One explanation can however be that the erosion area decreases but the intensity of the erosion at some particular place increases.

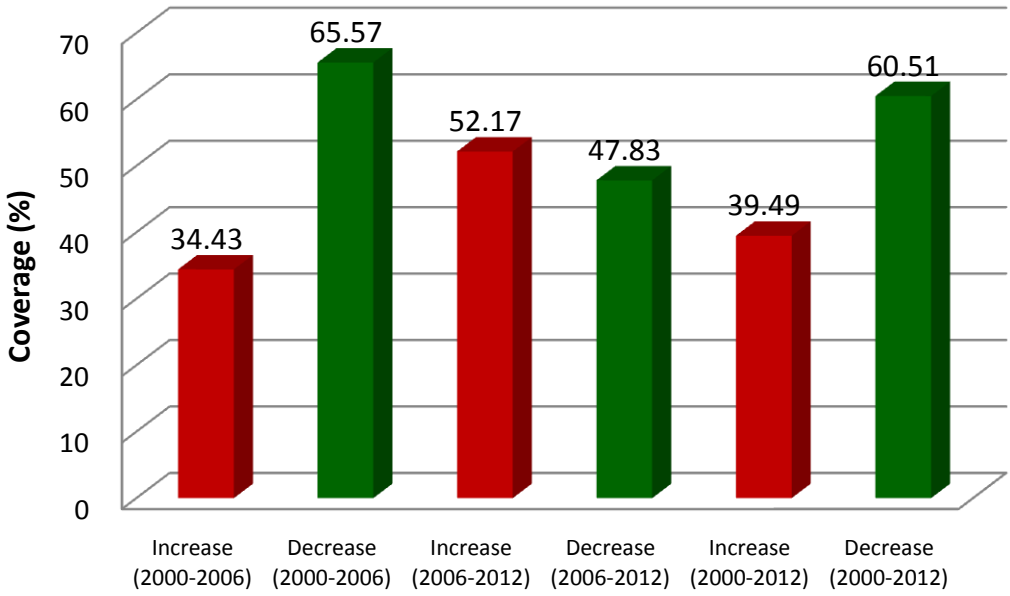

Figure 32. Coverage percentage of soil loss values increase and decrease from year 2000 to 2012.

5.5 Uncertainties and limitation

In general, due to the specific characteristics of study area, a mountainous area located in Mount Elgon region, finding the data which fulfill the requirement of RUSLE modeling is very difficult. In this study, most of the data are provided by local departments and researchers except for the ASTER remote sensing data. Due to lack of the data, the time series study was only carried out for three target years, 2000, 2006 and 2012. Mainly five key points are highlighted in following explanation for each of the original data.

In the result maps, some of the estimated soil loss values are very high, reaching 1454 $\mathrm{t\,ha^{-1}\,y^{-1}}$ using flow accumulation, and 6053 $\mathrm{t\,ha^{-1}\,y^{-1}}$ using flow length. The original DEM data is an interpolated 25 meters resolution raster map based on digitized contour lines. Due to 25 meters resolution, some sinks and breaks in the reality cannot be observed by DEM data and detected when using DEM data for calculating flow length and flow accumulation. In other words, the breaks in the flow pass may not be detected and the flow length and flow accumulation are overmuch calculated. This results in exaggerated estimations of flow lengths as well as flow accumulation, with correspondingly high LS-values. Additionally, because the DEM is interpolated from 10 meters contours map by local department, there are uncertainties when performing the interpolation.

Regarding precipitation, only data from four rainfall stations in the region were available for the three years 2000, 2006 and 2012. The precipitation maps for the entire study area were generated by running IDW interpolation with the data from these four points. Moreover, the location for the four climate stations used for interpolation is clustered in the eastern part of the study area. One can thus expect the interpolated precipitation values to be more accurate in the eastern part of the study area than the other areas. If the limitation of the original rainfall data can be solved and more rainfall data is available, the uncertainty from R-factor can be significantly reduced.

In the soil map, only five types of soil are detected in the study area, which does not have a good quality. In Uganda, soil mapping is still at a coarse scale, which also can be treated as a challenge to seek for good soil data. Anyway, with more detailed soil map can achieve a more accurate result. In addition, the method used to estimate K-factor is according to the color of the particular type of soil, which can be called as a rough estimation method and it is not accurate enough. In the study done by Xu et al. (2012), a more professional K-factor estimation method which refers to Sharpley & Williams (1990) is mentioned and presented. In order to apply this method, more detailed soil parameters are required, for instance, the subsoil sand fraction, the silt fraction, the clay fraction and topsoil carbon content in percentage. With more detailed soil information and using a more accurate estimation method, the K-factor values will be improved.

There are also uncertainties in the cover management factor which was estimated by the use of ASTER satellite images. There are mainly two sources generating the uncertainties, one is related to the temporal distribution of the satellite data, and the other related to cloud cover.

The satellite data it is supposed to befrom the same month and in summer time. The reason for this is that not only this period has the most vegetation cover, but also that it is the most serious erosion period due to rainy rains. However, the rainy season and the mountainous climate conditions result in extremely cloudy weather. It was impossible to find satellite data from the same month for different years. For the target year 2000, 2006, 2012, the images used in this study are from September 30, August 30 and June 27, respectively. We can thus expect more uncertainty in the image from July 2012. The land cover situation two month earlier than the other two target years may be significantly different.

The uncertainties relating to cloud are always a big problem when using remotely sensed data. In this study, all the images are influenced by cloud cover. Especially, in the year 2012, the cloud covers more than 12%. Because the shadow of the cloud has the negative effect on in NDVI and estimated C-factor values, the cloud was over-classified when carrying out the classification. The classified cloud area also contains the cloud shadow. Even though an over-classification was performed, some noise pixels still remained. In order to reduce the influence by these, a low pass 3x3 average filter was used to smooth the C-factor data layer.

The comparison made to adjust which method is better is mostly on qualitative aspect. Due to lack of the measurement field data, the quantitative evaluation is unable to be performed. However, from qualitative aspect with comparing with previous study, the results obtained by using flow accumulation are more prefer.

If all the problems mentioned above are solved and taken into consideration, by applying RUSLE model, the uncertainties in the estimated soil erosion results can be reduced significantly. In addition, more and better construction for the GIS database in this study field will also lead to increase the available data for time series study. Therefore, more detailed and continuous study can be performed.

6. Conclusion

This study attempts to find soil erosion patterns from year 2000 to 2012 due to climate and land cover changes based on estimating annual soil loss by applying two different versions of RUSLE model in Manafwa micro-catchment, Mount Elgon region, Uganda. The methodologies are based on previous studies, Bamutaze (2010), Pilesjö (1992) and Prasannakumar et al. (2012). Based on the results and the further analysis, the following conclusions can be drawn. Firstly, no significant trends in precipitation changes during the last decade are found. Even if there are reports of more intense and increasing amounts of rainfall in the area, this could not be verified, neither through analysis of climate data, nor trends in estimated soil loss. Secondly, the risk of soil erosion is not significantly different year 2012 compared to year 2000, and also no significant trends through target years. Thirdly, no specific trends or patterns in soil loss, precipitation and land cover have been found. Fourthly, even though there are no significant trends found, the mean annual soil loss values seem more sensitive to precipitation changes. Finally, the modified RUSLE model using flow accumulation instead of slope length is more preferred when estimating risk of soil erosion.

The study comes here, all the aims are achieved and all the research questions can be answered. As mentioned before, no significant trends and patterns of soil erosion are found. Over exploitation of land is probably compensated by improved agricultural management and no significant increase in precipitation.

The results obtained by this study are basically reliable, even if there may be some uncertainties and limitations during the processing of the study. For future studies working on this field, more targets years are suggested to be treated on. Furthermore, for a much better research, better datasets are needed. Thus, the construction and improvement of the database used for environmental analysis are expected to be implemented to reduce the uncertainties and limitations. Hopefully, more studies in this field will be carried out to estimate and solve land degradation problems, provide early warming service for the geologic hazard.

References

Angima, S.D., Stott, D.E., O'Neill, M.K., Ong, C.K. & Weesies, G.A. (2003). Soil erosion prediction using RUSLE for central Kenyan highland conditions. *Agriculture, Ecosystems and Environment 97(1-3),* 295-308.

Arnoldus, H.M.J. (1980). An approximation of the rainfall factor in the Universal Soil Loss Equation. In: De Boodt, M., Gabriels, D. (Eds.), Assessment of Erosion. Wiley, Chichester, UK, pp. 127-132.

Bamutaze, Y. (2010). *Patterns of water erosion and sediment loading in Manafwa catchment, Mt. Elgon, Eastern Uganda.* Makerere University.

Bamutaze, Y., Tenywa, M.M., Majaliwa, M.J.G., Vanacker, V., Bagoora, F., Magunda, M., Obando, J. & Ejiet Wasige, J. (2010). Infiltration characteristics of volcanic sloping soils on Mt. Elgon, Eastern Uganda. *Catena 80,* 122–130.

Bono, R. & Seiler, W. (1983). The soils of the Suke-Harerge Research Unit (Ethiopia). Classification, Morphology and Ecology. With Map 1: 5000. Research Report 2 with Supplement, Soil Conservation Research Project, Addis Abeba, 95 pp.

Bono, R. & Seiler, W. (1984). The soils of the Andit Tid Research Unit (Ethiopia). Classification, Morphology and Ecology. With Map 1: 10000. Research Report 3 with Supplement, Soil Conservation Research Project, Addis Abeba, 80 pp.

Brunner, A.C., Park, S.J., Ruecker, G.R., Dikau, R. & Vlek, P.L.G. (2004). Catenary soil development influencing erosion susceptibility along a hillslope in Uganda. *Catena 58,* 1-22.

Chretien, J., King, D., Jamagne, M. & Hardy, R. (1994). Conception of soil spatial organisation model and soil functioning unit in GIS for land use and conservation. *15th World Congress of Soil Science, Acapulco 6,* 296-297.

Claessens, L., Knapen, A., Kitutu, M.G., Poesen, J., & Deckers, J.A. (2007). Modelling landslide hazard, soil redistribution and sediment yield of landslides on the Ugandan footslopes of Mount Elgon. *Geomorphology 90,* 23-35.

De Meyer, A., Poesen, J., Isabirye, M., Deckers, J. & Raes, D. (2011). Soil erosion rates in tropical villages: A case study from Lake Victoria Basin, Uganda. *Catena 84,* 89-98.

Fistikoglu, O. & Harmancioglu, N.B. (2002). Integration of GIS with USLE in assessment of soil erosion. *Water Resources Management 16,* 447-467.

Fu, B. & Gulinck, H. (1994). Land evaluation in an area of severe erosion. The loess plateau of China. *Land Degrad. Rehabil 5 (1),* 33-40.

Fu, B.J., Zhao, W.W., Chen, L.D., Zhang, Q.J., Lu, Y.H., Gulinck, H. & Poesen, J. (2005). Assessment of soil erosion at large watershed scale using RUSLE and GIS: A case study in the Loess Plateau of China. *Land Degradation & Development 16,* 73-85.

Hansen, A.J., Dale, R.P., Flather, V.H., Iverson, C. & Currie, L. (2001). Global change in forests. Responses of species, communities and biomass. *Bioscience 51,* 765-779.

Hoyos, N. (2005). Spatial modeling of soil erosion potential in a tropical watershed of the Colombian Andes. *Catena 63 (1),* 85-108.

Hudson, N. (1981). *Soil Conservation.* Batsford Academic and Educational. London.

Isabirye, M., Mbeera, D., Ssali, H., Magunda, M. & Lwasa, J. (2004). Soil resource information and linkages to agricultural production. *Uganda Journal of Agricultural Science 9.*

ISRIC (World Soil Information) (2013). [Online], available at: http://www.isric.org/isric/webdocs/docs//major_soils_of_the_world/set6/nt/nitisol.pdf (Accessed: May 26, 2013).

Jasrotia, A.S. & Singh, R. (2006). Modeling runoff and soil erosion in a catchment area, using the GIS, in the Himalayan region, India. *Environmental Geology 51,* 29-37.

Karydas, C.G., Sekuloska, T. & Silleos, G.N. (2009). Quantification and site-specification of the support practice factor when mapping soil erosion risk associated with olive plantations in the Mediterranean island of Crete. *Environmental Monitoring and Assessment 149,* 19-28.

Kitutu, M.G., Muwanga, A., Poesen, J. & Deckers, J. (2009). Influence of soil properties on landslide occurrence in Bududa District, Eastern Uganda. *African Journal of Agricultural Research 4,* 611-620.

Knapen, A., Kitutu, M.G., Poesen, J., Breugelmans, W., Deckers, J. & Muwanga, A. (2006). Landslides in a densely populated county at the footslopes of Mount Elgon (Uganda): Characteristics and causal factors. *Geomorphology 73,* 149-165.

Kouli, M., Soupios, P. & Vallianatos, F. (2009). Soil erosion prediction using the Revised Universal Soil Loss Equation (RUSLE) in a GIS framework, Chania, Northwestern Crete, Greece. *Environmental Geology 57,* 483-497.

Lung, T. & Schaab, G. (2010). A comparative assessment of land cover dynamics of three protected forest areas in tropical East Africa. *Environmental Monitoring and Assessment 161,* 531–548.

Millward, A.A. & Mersey, J.E. (1999). Adapting the RUSLE to model soil erosion potential in a mountainous tropical watershed. *Catena 38(2),* 109-129.

Moore, I.D. & Burch, G.J. (1986a). Physical basis of the length slope factor in the Universal Soil Loss Equation. *Soil Science Society of America 50 (5),* 1294-1298.

Moore, I.D. & Burch, G.J., (1986b). Modeling erosion and deposition. Topographic effects. *Transactions of American Society of Agriculture Engineering 29 (6),* 1624-1630.

Mugagga, F., Kakembo, V., Buyinza, M. (2012). Land use changes on the slopes of Mount Elgon and the implications for the occurrence of landslides. *Catena 90,* 39-46.

NEMA (1998). *State of the environment report for Uganda.* National Environmental Management Authority. NEMA, Kampala.

Nekhay, O., Arriaza, M. & Boerboom, L. (2009). Evaluation of soil erosion risk using Analytic Network Process and GIS: A case study from Spanish mountain olive plantations. *Journal of Environmental Management 90,* 3091-3104.

Omuto, C.T. (2008). Assessment of soil physical degradation in Eastern Kenya by use of a sequential soil testing protocol. *Agriculture, Ecosystems and Environment 128,* 199-211.

Park, S., Oh, C., Jeon, S. & Jung, H., Choi, C. (2011). Soil erosion risk in Korean watersheds, assessed using the revised universal soil loss equation. *Journal of Hydrology 399 (3-4),* 263-273.

Pilesjö, P. (1992). *GIS and remote sensing for soil erosion studies in semi-arid environments, estimation of soil erosion parameters at different scales.* Lund University Press. Department of physical geography, the University of Lund, Sweden.

Prasannakumar, V., Vijith, H., Abinod, S. & Geetha, N. (2012). Estimation of soil erosion risk within a small mountainous sub-watershed in Kerala, India, using Revised Universal Soil Loss Equation (RUSLE) and geo-information technology. *Geoscience Frontiers 3(2),* 209-215.

Rafaelli, S.G., David R. Montgomery, D.R. & Greenberg, H.M. (2001). A comparison of thematic mapping of erosional intensity to GIS-driven process models in an Andean drainage basin. *Journal of Hydrology 244,* 33-42.

Renard, K.G., Foster, G.R., Weesies, G.A., McCool, D.K. & Yoder, D.C. (1997). Predicting Soil Erosion by Water: A Guide to Conservation Planning with the Revised Universal Soil Loss Equation (RUSLE). *Agriculture Handbook 703,* 1-251.

Scott, P. (1994). *An assessment of natural resource use by communities from Mt. Elgon National Park.* UNDP/Technical Report No. 15, 1994.

Sharpley, A.N. & Williams, J.R. (1990). *EPIC-Erosion/Productivity Impact Calculator: 1. Model Documentation.* US Department of Agriculture Technical Bulletin No. 1768, Washington DC, pp. 235.

Soini, E. (2005). Land use change patterns and livelihood dynamics on the slopes of Mt Kilimanjaro, *Tanzania. Agricultural Systems 85,* 306-323.

Tian, Y.C., Zhou, Y.M., Wu, B.F. & Zhou, W.F. (2009). *Risk Assessment of Water Soil Erosion in Upper Basin of Miyun Reservoir, vol. 57.* Environmental Geology, Beijing, China, pp. 937-942.

UNEP (2004). *Global environment outlook scenario framework. Background Paper for UNEP's Third Global Environment Outlook Report (GEO-3).* United Nations Environment Programme, Nairobi.

Van der Knijff, J.M., Jones, R.J.A. & Montanarella, L. (2000). *Soil Erosion Risk Assessment in Europe.* EUR 19044 EN. Office for Official Publications of the European Communities, Luxembourg, p. 34.

Van Heist, M. (1994). Accompanying report with the Land unit map of Mount Elgon National Park. Mount Elgon Conservation and Development Project. *Kampala. 83.*

Wasige, E.J., Tenywa, M.M., Majaliwa, J.G., Bamutaze, Y., Bekunda, M.A., & Lal, R. (2007). *Geo-spatial analysis for targeted natural resource management in the Mt. Elgon areas of Uganda.* Soil Science Society of East Africa, Masaka.

Wesche, K. (2002). The high-altitude environment of Mt. Elgon (Uganda/Kenya) - Climate, vegetation and the impact of fire. *Ecotropical Monographs 2,* 1-253.

Wischmeier, W.H. (1976). Use and misuse of the universal soil loss equation. J*ournal of Soil and Water Conservation 31(1),* 5-9.

Wischmeier, W.H. & Smith, D.D., (1978). *Predicting Rainfall Erosion Losses - A Guide to Conservation Planning. Agriculture Handbook No. 537.* US Department of Agriculture Science and Education Administration, Washington, DC, USA, pp. 168.

Xu, L., Xu, X. & Meng, X. (2012). Risk assessment of soil erosion in different rainfall scenarios by RUSLE model coupled with Information Diffusion Model: A case study of Bohai Rim, China. *Catena 100,* 74-82.

Zhang, X., Wu, B., Ling, F., Zeng, Y., Yan, N. & Yuan, C. (2010). Identification of priority areas for controlling soil erosion. *Catena 83,* 76-86.

Zhou, P., Luukkanen, O., Tokola, T. & Nieminen, J. (2008). Effect of vegetation cover on soil erosion in a mountainous watershed. *Catena 75(3),* 319-325.

Appendix

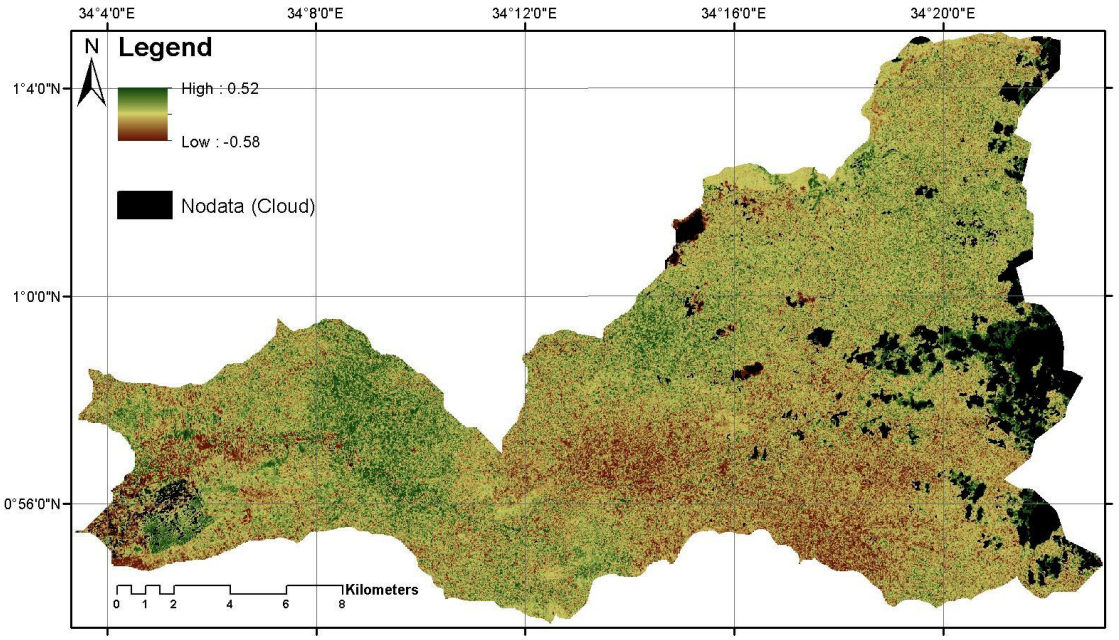

Figure 1. The map of NDVI change between year 2000 and 2006.

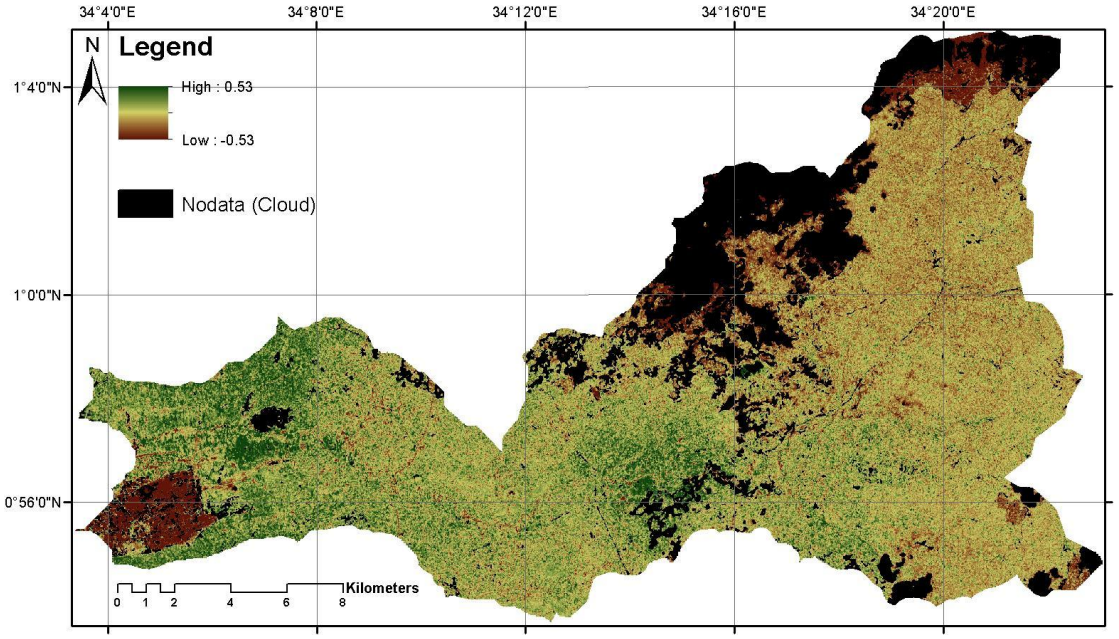

Figure 2. The map of NDVI change between year 2006 and 2012.

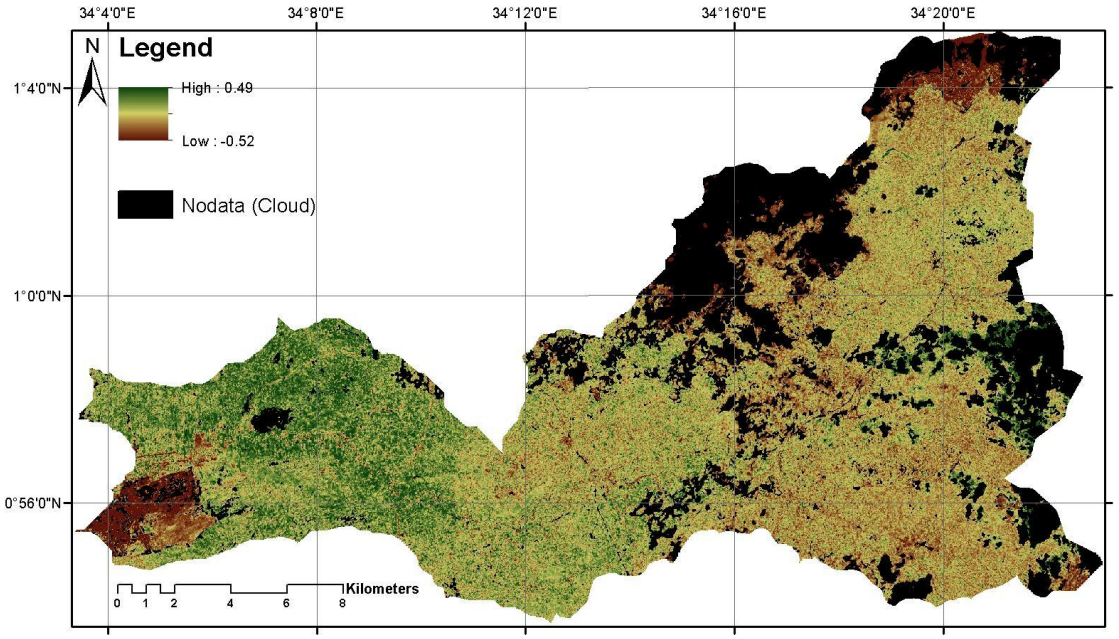

Figure 3. The map of NDVI change between year 2000 and 2012.

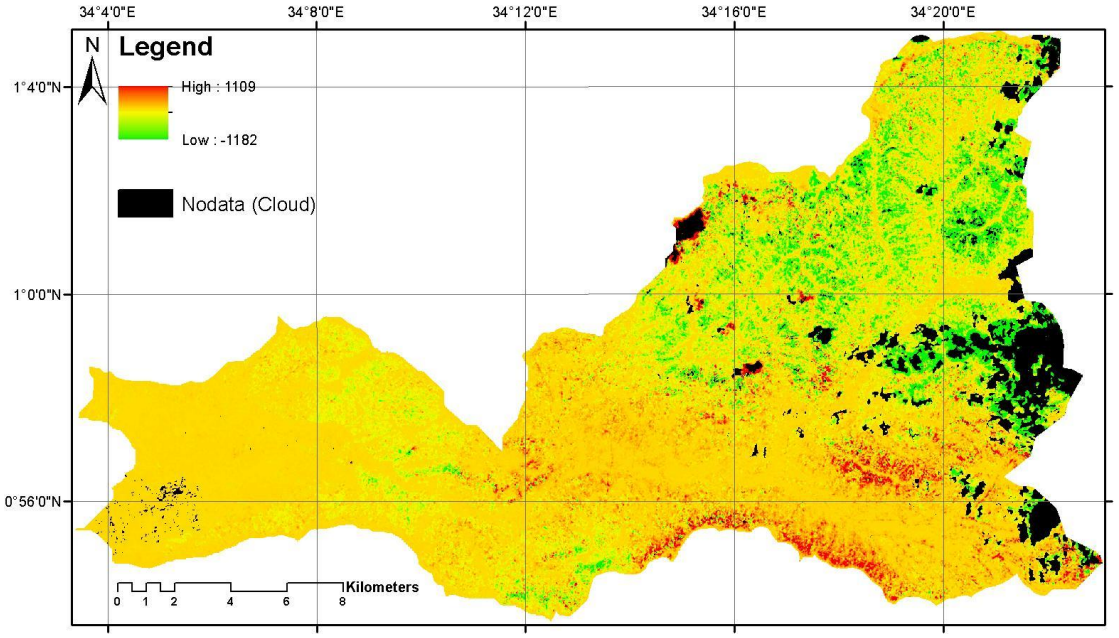

Figure 4. The map of soil loss change between year 2000 and 2006.

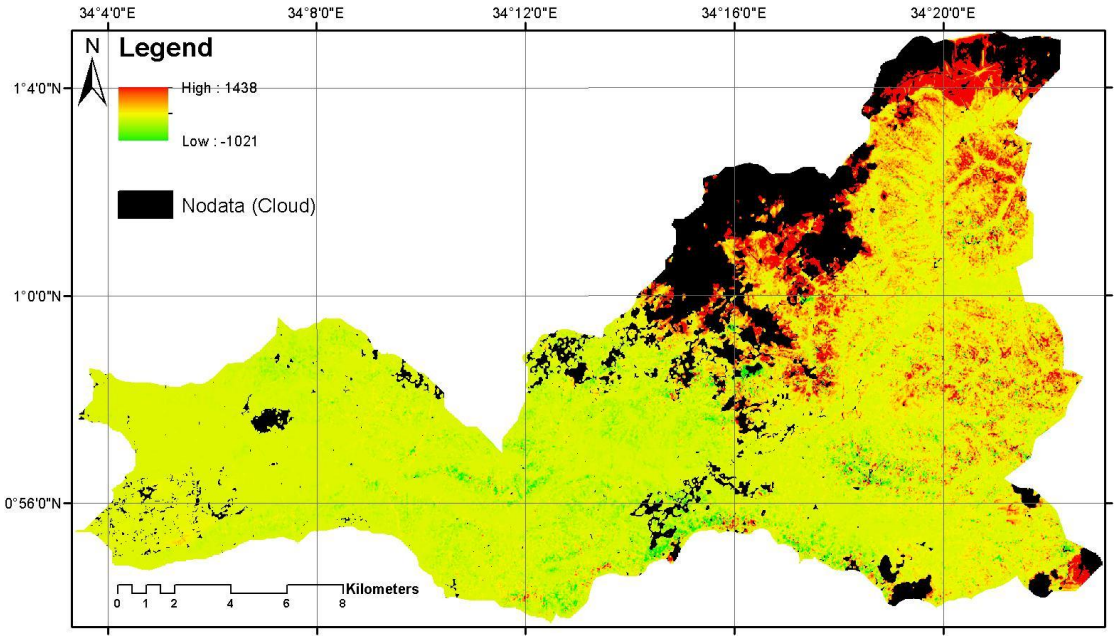

Figure 5. The map of soil loss change between year 2006 and 2012.

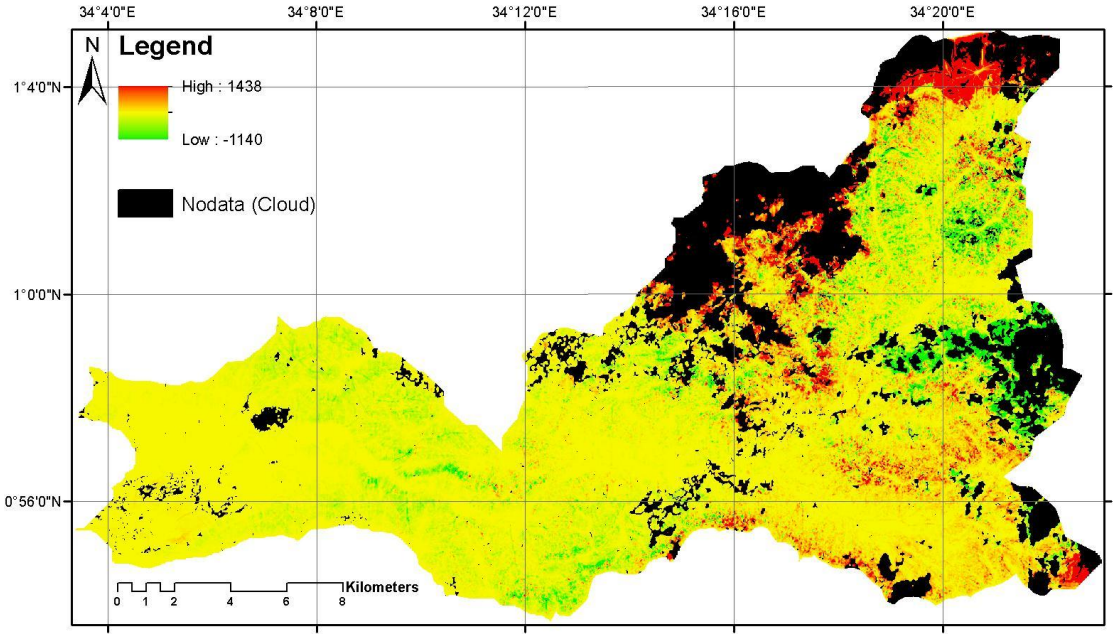

Figure 6. The map of soil loss change between year 2000 and 2012.

Institutionen för naturgeografi och ekosystemvetenskap, Lunds Universitet.

Student examensarbete (Seminarieuppsatser). Uppsatserna finns tillgängliga på institutionens geobibliotek, Sölvegatan 12, 223 62 LUND. Serien startade 1985. Hela listan och själva uppsatserna är även tillgängliga på LUP student papers (www.nateko.lu.se/masterthesis) och via Geobiblioteket (www.geobib.lu.se)

The student thesis reports are available at the Geo-Library, Department of Physical Geography and Ecosystem Science, University of Lund, Sölvegatan 12, S-223 62 Lund, Sweden. Report series started 1985. The complete list and electronic versions are also electronic available at the LUP student papers (www.nateko.lu.se/masterthesis) and through the Geo-library (www.geobib.lu.se)

230 Cléber Domingos Arruda (2011) Developing a Pedestrian Route Network Service (PRNS)
231 Nitin Chaudhary (2011) Evaluation of RCA & RCA GUESS and estimation of vegetation-climate feedbacks over India for present climate
232 Bjarne Munk Lyshede (2012) Diurnal variations in methane flux in a low-arctic fen in Southwest Greenland
233 Zhendong Wu (2012) Dissolved methane dynamics in a subarctic peatland
234 Lars Johansson (2012) Modelling near ground wind speed in urban environments using high-resolution digital surface models and statistical methods
235 Sanna Dufbäck (2012) Lokal dagvattenhantering med grönytefaktorn
236 Arash Amiri (2012)Automatic Geospatial Web Service Composition for Developing a Routing System
237 Emma Li Johansson (2012) The Melting Himalayas: Examples of Water Harvesting Techniques
238 Adelina Osmani (2012) Forests as carbon sinks - A comparison between the boreal forest and the tropical forest
239 Uta Klönne (2012) Drought in the Sahel – global and local driving forces and their impact on vegetation in the 20th and 21st century
240 Max van Meeningen (2012) Metanutsläpp från det smältande Arktis
241 Joakim Lindberg (2012) Analys av tillväxt för enskilda träd efter gallring i ett blandbestånd av gran och tall, Sverige
242 Caroline Jonsson (2012) The relationship between climate change and grazing by herbivores; their impact on the carbon cycle in Arctic environments
243 Carolina Emanuelsson and Elna Rasmusson (2012) The effects of soil erosion on nutrient content in smallholding tea lands in Matara district, Sri Lanka
244 John Bengtsson and Eric Torkelsson (2012) The Potential Impact of Changing Vegetation on Thawing Permafrost: Effects of manipulated vegetation on summer ground temperatures and soil moisture in Abisko, Sweden

245 Linnea Jonsson (2012). Impacts of climate change on Pedunculate oak and Phytophthora activity in north and central Europe
246 Ulrika Belsing (2012) Arktis och Antarktis förändrliga havsistäcken
247 Anna Lindstein (2012) Riskområden för erosion och näringsläckage i Segeåns avrinningsområde
248 Bodil Englund (2012) Klimatanpassningsarbete kring stigande havsnivåer i Kalmar läns kustkommuner
249 Alexandra Dicander (2012) GIS-baserad översvämningskartering i Segeåns avrinningsområde
250 Johannes Jonsson (2012) Defining phenology events with digital repeat photography
251 Joel Lilljebjörn (2012) Flygbildsbaserad skyddszonsinventering vid Segeå
252 Camilla Persson (2012) Beräkning av glaciärers massbalans – En metodanalys med fjärranalys och jämviktslinjehöjd över Storglaciären
253 Rebecka Nilsson (2012) Torkan i Australien 2002-2010 Analys av möjliga orsaker och effekter
254 Ning Zhang (2012) Automated plane detection and extraction from airborne laser scanning data of dense urban areas
255 Bawar Tahir (2012) Comparison of the water balance of two forest stands using the BROOK90 model
256 Shubhangi Lamba (2012) Estimating contemporary methane emissions from tropical wetlands using multiple modelling approaches
257 Mohammed S. Alwesabi (2012) MODIS NDVI satellite data for assessing drought in Somalia during the period 2000-2011
258 Christine Walsh (2012) Aerosol light absorption measurement techniques: A comparison of methods from field data and laboratory experimentation
259 Jole Forsmoo (2012) Desertification in China, causes and preventive actions in modern time
260 Min Wang (2012) Seasonal and inter-annual variability of soil respiration at Skyttorp, a Swedish boreal forest
261 Erica Perming (2012) Nitrogen Footprint vs. Life Cycle Impact Assessment methods – A comparison of the methods in a case study.
262 Sarah Loudin (2012) The response of European forests to the change in summer temperatures: a comparison between normal and warm years, from 1996 to 2006
263 Peng Wang (2012) Web-based public participation GIS application – a case study on flood emergency management
264 Minyi Pan (2012) Uncertainty and Sensitivity Analysis in Soil Strata Model Generation for Ground Settlement Risk Evaluation
265 Mohamed Ahmed (2012) Significance of soil moisture on vegetation greenness in the African Sahel from 1982 to 2008
266 Iurii Shendryk (2013) Integration of LiDAR data and satellite imagery for biomass estimation in conifer-dominated forest
267 Kristian Morin (2013) Mapping moth induced birch forest damage in northern Sweden, with MODIS satellite data
268 Ylva Persson (2013) Refining fuel loads in LPJ-GUESS-SPITFIRE for wet-dry areas - with an emphasis on Kruger National Park in South Africa
269 Md. Ahsan Mozaffar (2013) Biogenic volatile organic compound emissions from Willow trees
270 Lingrui Qi (2013) Urban land expansion model based on SLEUTH, a case

study in Dongguan City, China

271 Hasan Mohammed Hameed (2013) Water harvesting in Erbil Governorate, Kurdistan region, Iraq - Detection of suitable sites by using Geographic Information System and Remote Sensing

272 Fredrik Alström (2013) Effekter av en havsnivåhöjning kring Falsterbohalvön.

273 Lovisa Dahlquist (2013) Miljöeffekter av jordbruksinvesteringar i Etiopien

274 Sebastian Andersson Hylander (2013) Ekosystemtjänster i svenska agroforestrysystem

275 Vlad Pirvulescu (2013) Application of the eddy-covariance method under the canopy at a boreal forest site in central Sweden

276 Malin Broberg (2013) Emissions of biogenic volatile organic compounds in a Salix biofuel plantation – field study in Grästorp (Sweden)

277 Linn Renström (2013) Flygbildsbaserad förändringsstudie inom skyddszoner längs vattendrag

278 Josefin Methi Sundell (2013) Skötseleffekter av miljöersättningen för natur- och kulturmiljöer i odlingslandskapets småbiotoper

279 Kristín Agustsdottír (2013) Fishing from Space: Mackerel fishing in Icelandic waters and correlation with satellite variables

280 Cristián Escobar Avaria (2013) Simulating current regional pattern and composition of Chilean native forests using a dynamic ecosystem model

281 Martin Nilsson (2013) Comparison of MODIS-Algorithms for Estimating Gross Primary Production from Satellite Data in semi-arid Africa

282 Victor Strevens Bolmgren (2013) The Road to Happiness – A Spatial Study of Accessibility and Well-Being in Hambantota, Sri Lanka

283 Amelie Lindgren (2013) Spatiotemporal variations of net methane emissions and its causes across an ombrotrophic peatland - A site study from Southern Sweden

284 Elisabeth Vogel (2013) The temporal and spatial variability of soil respiration in boreal forests - A case study of Norunda forest, Central Sweden

285 Cansu Karsili (2013) Calculation of past and present water availability in the Mediterranean region and future estimates according to the Thornthwaite water-balance model

286 Elise Palm (2013) Finding a method for simplified biomass measurements on Sahelian grasslands

287 Manon Marcon (2013) Analysis of biodiversity spatial patterns across multiple taxa, in Sweden

288 Emma Li Johansson (2013) A multi-scale analysis of biofuel-related land acquisitions in Tanzania - with focus on Sweden as an investor

289 Dipa Paul Chowdhury (2013) Centennial and Millennial climate-carbon cycle feedback analysis for future anthropogenic climate change

290 Zhiyong Qi (2013) Geovisualization using HTML5 - A case study to improve animations of historical geographic data

291 Boyi Jiang (2013) GIS-based time series study of soil erosion risk using the Revised Universal Soil Loss Equation (RUSLE) model in a micro-catchment on Mount Elgon, Uganda